

Interference Reduction in Multi-Cell Massive MIMO Systems I: Large-Scale Fading Precoding and Decoding

Alexei Ashikhmin¹, Thomas L. Marzetta¹, and Liangbin Li²

¹Bell Laboratories Alcatel-Lucent, 600 Mountain Ave, Murray Hill, NJ 07974.

²University of California, Irvine, CA 92617.

Abstract—A wireless massive MIMO system entails a large number (tens or hundreds) of base station antennas serving a much smaller number of users, with large gains in spectral-efficiency and energy-efficiency compared with conventional MIMO technology. Until recently it was believed that in multi-cellular massive MIMO system, even in the asymptotic regime, as the number of service antennas tends to infinity, the performance is limited by directed inter-cellular interference. This interference results from unavoidable re-use of reverse-link training sequences (pilot contamination) by users in different cells.

We devise a new concept that leads to the effective elimination of inter-cell interference in massive MIMO systems. This is achieved by outer multi-cellular precoding, which we call Large-Scale Fading Precoding (LSFP). The main idea of LSFP is that each base station linearly combines messages aimed to users from different cells that re-use the same training sequence. Crucially, the combining coefficients depend only on the *slow-fading coefficients* between the users and the base stations. Each base station independently transmits its LSFP-combined symbols using conventional linear precoding that is based on estimated *fast-fading coefficients*. Further, we derive estimates for downlink and uplink SINRs and capacity lower bounds for the case of massive MIMO systems with LSFP and a finite number of base station antennas.

I. INTRODUCTION

Multiple-input multiple-output (MIMO) technology has been a subject of intensive studies during the last two decades. This technology became a part of many wireless standards since it can significantly improve the efficiency and reliability of wireless systems. Initially, research in this area was focused on the point-to-point communication scenario, when two devices are equipped with multiple antennas communicate to each other. In recent years, the focus has shifted to multi-user multiple-input multiple-output (MU-MIMO) systems, in which a base station is equipped with multiple antennas and simultaneously serves a multiplicity of autonomous users. These users can be cheap single-antenna devices and most of the expensive equipment is needed only at base stations. Another advantage of MU-MIMO systems is their high multi-user diversity, which allows making the system performance more robust to the propagation environment than in the case of point-to-point MIMO case. As a result, MU-MIMO has become an integral part of communications standards, such as 802.11 (WiFi), 802.16 (WiMAX), LTE, and is progressively being deployed throughout the world.

In most modern MU-MIMO systems, base stations have only a few, typically fewer than 10, antennas, which results in relatively modest spectral efficiency and precludes a rapid increase in data rates, as well as higher user density required in the next generation cellular networks. This, along with the GreenTouch initiative to decrease the power consumption in communication networks, motivated extensive research on Massive MIMO systems, where each base station is equipped with a significantly larger number of antennas, e.g., 64 or more.

In [1] and [3], Marzetta used asymptotic arguments based on random matrix theory to show that the effects of additive noise and intra-cell interference, and the required transmitted energy per bit vanishes as the number of base station antennas grows to infinity. Furthermore, simple linear signal processing approaches, such as matched filter precoding/detection, can be used to achieve these advantages.

Another important advantage of massive MIMO system is their energy efficiency. In [4], it is shown that the transmit power scales down linearly with the number of antennas. The high energy efficiency of massive MIMO systems is very important since the large energy consumption can be one of the main technical issues in future wireless networks [5], [6].

Because of the above advantages, in recent years, massive MIMO systems attracted significant attention of the research community. Understanding signal processing, information theoretic properties, optimization of parameters, and other aspects of massive MIMO system become subjects of intensive studies. The articles [7], [8], and [9] present a good introduction into this area, including fundamental information theoretical limits, antenna and propagation aspects, design of precoder/decoder, and other technical issues.

In this work, we consider one of the most important and interesting problems of massive MIMO systems - pilot contamination. In [3] (see also [10] and [11]), Marzetta derived estimates for SINR values in a non-cooperative cellular network in the asymptotic regime when the number of base station antennas tends to infinity. He showed that in this regime not all interference vanishes, and therefore, SINR does not grow indefinitely. The reason for this is that, unless all users in the network use mutually orthogonal training sequences (pilots), the training sequences transmitted by different users contaminate each other. As a result, the estimates of channel

state information made at a base station are biased toward users located in other cells. This effect is called *pilot contamination problem*. The pilot contamination causes the inter-cell interference that is proportional to the number of base station antennas.

A number of techniques were proposed for mitigation the pilot contamination. The numerical results obtained in [10],[11], and [13] show that these techniques provide breakthrough data transmission rates for noncooperative cellular networks. Advanced network MIMO systems that allow some collaboration between base stations were proposed recently in [14]. Unfortunately, in all these techniques SINR values remain finite and do not grow indefinitely with the number of base station antennas M .

In [15] and [16], the authors proposed massive MIMO systems with limited collaboration between base stations and an outer multi-cellular precoding. This outer-cellular precoding is based only on the use of large-scale fading coefficients between base stations and users. Since large-scale fading coefficients do not depend on antenna index and frequency, the number of them is relatively small - only one coefficient for each pair of a base station and an user. In addition, these coefficients change slowly over time. Thus, the proposed outer-cellular precoding does not require extensive traffic between base stations and/or a network controller. In the asymptotic regime, as M tends to infinity, this outer-cellular precoding allows one to construct interference and noise free multi-cell massive MIMO systems with frequency reuse one. In this work, we present these results in full details with rigorous proofs and extend them to the real life scenario when the number of base station antennas is finite.

In [15] and [16], the main goal for designing the outer-cellular precoding was cancelation of the interference caused by the pilot contamination, and therefore we called it *pilot contamination precoding*. It happened, however, that in the regime of a finite number of antennas, other sources of interference, caused not by pilot contamination, can not be ignored. The outer-cellular precoding allows one to efficiently mitigate these sources of interference. For this reason, we decided that *large-scale fading precoding* is a better name for it.

The paper is organized as follows. First, in Section II, we describe our system model, network assumptions, and TDD protocol. Then, in Section III-A, we explain the pilot contamination problem and why inter-cell interference does not vanish as the number of base station antennas grows. In Sections III-B and III-C we propose large-scale fading precoding and decoding protocols and show that in the asymptotic regime, as the number of base station antennas tends to infinity, these protocols allow construction of interference and noise free massive MIMO systems. In Section III-D, we briefly outline an approach for estimation of large-scale fading coefficients. In Section IV, we analyze LSFP and LSF in the regime of a finite number of base station antennas. In particular, in Section IV-A and IV-E, we derive estimates for downlink and uplink SINRs and the capacity of massive MIMO systems with large-scale precoding and decoding respectively. Further, in IV-B, we consider two cases: when LSFP is not used,

and when Zero-Forcing LSFP is used. In IV-C, we formulate an optimization problem for designing efficient LSFP and in IV-D, we present simulation results for Zero-Forcing LSFP for different number of base station antennas.

II. SYSTEM MODEL

We consider a two-dimensional hexagonal cellular network composed of L hexagonal cells with one base station and K users in each cell. Each base station is equipped with M omnidirectional antennas and each user has a single omnidirectional antenna. We further assume that Orthogonal Frequency-Division Multiplexing (OFDM) is used and that in a given subcarrier we have a flat-fading channel.

The throughput of 95% of users can be improved by using massive MIMO system with frequency reuse factor greater than one [3]. Alternatively one can improve the throughput by using a pilot reuse factor greater than one [17]. For instance, a pilot reuse factor of seven allows assigning orthogonal pilots to users in two concentric rings of cells, at the expense of a longer training time. Similarly, the results presented in this work can be further improved by applying a frequency reuse factor or pilot reuse factor different from one. However, to make presentation shorter, we will consider only the case of frequency reuse and pilot reuse one. Thus the entire frequency band is used for downlink and uplink transmissions by all base stations and all users, and the length of the pilot sequences is equal to the number of users in one cell.

A. Channel Model

For a given subcarrier, we denote by

$$g_{mj}^{[kl]} = \sqrt{\beta_j^{[kl]}} h_{mj}^{[kl]} \quad (1)$$

the *channel (propagation) coefficient* between the m -th antenna of the j -th base station and the k -th terminal of the l -th cell, Fig. 1. The first factor in (1) is the large-scale fading coefficient $\beta_j^{[kl]} \in \mathbb{R}^+$ and the second factor is the small-scale fading coefficient $h_{mj}^{[kl]} \in \mathbb{C}$.

A large-scale fading coefficient depends on the shadowing and distance between the corresponding user and base station. Typically, the distance between a user and base station is significantly larger than the distance between base station antennas. For this reason, the standard assumption is that the large-scale fading coefficients do not depend on the antenna index m of a given base station. We also assume that these coefficients are constant across the used frequency band, i.e., that they do not depend on OFDM subcarrier index. Thus there is only one large-scale fading coefficients for each pair of a user and a base station. A detailed model for the large-scale fading coefficients will be given in Part II of the paper [2].

In contrast, the small-scale fading coefficients depend on both the antenna and subcarrier indices. Hence, if N is the number of OFDM subcarriers, then for each pair of a user and base station there are about NM small-scale fading coefficients. In what follows, we consider only one OFDM subcarrier and so we do not write the subcarrier index for small-scale fading coefficients. For small-scale fading coefficients,

we assume Rayleigh fading model, i.e., $h_{mj}^{[kl]} \sim \mathcal{CN}(0, 1)$ and for any $(m, j, k, l) \neq (u, i, n, v)$ the coefficients $h_{mj}^{[kl]}$ and $h_{ui}^{[nv]}$ are independent. From the above assumptions it follows that for any $(j, k, l) \neq (i, n, v)$ the vectors $\mathbf{h}_j^{[kl]}$ and $\mathbf{h}_i^{[nv]}$ (similarly $\mathbf{g}_j^{[kl]}$ and $\mathbf{g}_i^{[nv]}$) are independent.

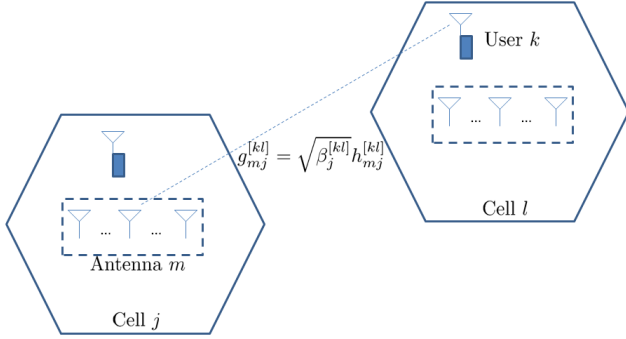


Fig. 1. The channel coefficient $g_{mj}^{[kl]}$ between the m -th antenna of the j -th cell and the k -th terminal in the l -th cell

The small-scale fading coefficients between the j -th base station and the k -th user in the l -th cell form *small-scale fading vector*

$$\mathbf{h}_j^{[kl]} = \left(h_{1j}^{[kl]}, h_{2j}^{[kl]}, \dots, h_{Mj}^{[kl]} \right)^T \in \mathbb{C}^{M \times 1}.$$

The channel coefficients between the j -th base station and the k -th user in the l -th cell form *channel vector*

$$\mathbf{g}_j^{[kl]} = \left(g_{1j}^{[kl]}, g_{2j}^{[kl]}, \dots, g_{Mj}^{[kl]} \right)^T = \sqrt{\beta_j^{[kl]}} \mathbf{h}_j^{[kl]} \in \mathbb{C}^{M \times 1}.$$

Since small-scale fading coefficients are i. i. d., we have $\mathbf{h}_j^{[kl]} \sim \mathcal{CN}(0, \mathbf{I}_M)$ and $\mathbf{g}_j^{[kl]} \sim \mathcal{CN}(0, \beta_j^{[kl]} \mathbf{I}_M)$.

We further assume a block fading model, that is, that small-scale coefficients $h_j^{[kl]}$ stay constant during coherence blocks of T OFDM symbols. The small-scale fading coefficients in different coherence blocks are assumed to be independent. Similarly, we assume that large-scale fading coefficients $\beta_j^{[kl]}$ stay constant during large-scale coherence blocks of T_β OFDM symbols. Typically T_β is significantly larger than T (at the end of Section III we discuss this in more details). For different large-scale coherence blocks coefficients $\beta_j^{[kl]}$ are assumed being independent.

Since large-scale fading coefficients stay constant for long coherence blocks and the number of these coefficients is relatively small (for each pair of base station and mobile there is only one large-scale fading coefficient) throughout the paper we use the following

Network Assumptions I:

- 1) We assume that the j -th base station can accurately estimate and track large-scale fading coefficients $\beta_j^{[kl]}$ with $k = 1, K$ and $l = 1, L$.
- 2) If $\epsilon_j^{[kj]}$ is a quantity that depends only on large-scale fading coefficients we assume that the j -th base station has means to forward it to the k -th user in the j -th cell.

Throughout the paper, in our analysis of communication protocols we will not take into account the resources needed for implementing the above assumptions.

Finally, we assume reciprocity between uplink and downlink channels, i.e., $\beta_j^{[kl]}$ and $\mathbf{h}_{mj}^{[kl]}$ are the same for these channels. The reciprocity, up to high accuracy, can be achieved with proper calibration of hardware components, e.g., the transmitted power amplifier and the received low-noise amplifier.

B. Time-Division Duplexing Protocol

We consider a wireless network, where each cell has K users enumerated by index k from 1 to K . In each cell, the same set of K orthonormal training sequences $\mathbf{r}^{[k]} \in \mathbb{C}^{\tau \times 1}$ ($\mathbf{r}^{[k]\dagger} \mathbf{r}^{[i]} = \delta_{ki}$) are assigned to the users. The sequence $\mathbf{r}^{[k]}$ is assigned to the k -th user. Since small-scale fading vectors are mutually independent for different coherence blocks, we have to assume that $\tau < T$. Since the number of orthogonal τ -tuples can not exceed τ , we also have $K \leq \tau$.

The assumption that the same set of training sequences is used in all cells is justified in the following. If users move fast, the coherence block is short, that is, T is small. Hence τ , the training time, should be also small. Therefore, it is reasonable to assume that we can assign orthogonal training sequences to users within one cell, but there are not enough orthogonal training sequences for users from different cells. Thus, we have to reuse the same training sequences in all cells.

There is an alternative scheme in which different sets of training sequences are used in different cells. Thus, in the l -th cell the orthonormal sequences $\mathbf{r}_l^{[k]} \in \mathbb{C}^{\tau \times 1}$, $k = 1, K$, are used. In this case, however, the training sequences from different cells are still nonorthogonal, that is, for generic $\mathbf{r}_l^{[k]}$ and $\mathbf{r}_n^{[i]}$, we have $|\mathbf{r}_l^{[k]\dagger} \mathbf{r}_n^{[i]}| > 0$. Our estimates show that such a scheme would achieve performance similar to the scheme with the same set of training sequences in all cells. At the same time, the analysis becomes more complex. For this reason, in this paper, we do not consider the alternative scheme, which, however, could be done in future works.

The Time-Division Duplexing (TDD) protocol consists of six steps. The last four steps, that are conducted during each coherence block, are shown in Fig.2.

Time-Division Duplexing Protocol

- 1) In the beginning of each large-scale coherence block (of duration T_β OFDM symbols) the j -th base station estimates the large-scale fading coefficients $\beta_j^{[kl]}$, $k = 1, K$, $l = 1, L$.
- 2) Next, the j -th base station transmits to K mobiles located in the j -th cell the quantities

$$\epsilon_j^{[kj]} = \frac{\sqrt{M \rho_f \rho_r \tau} \beta_j^{[kj]}}{\left(1 + \sum_{s=1}^L \rho_r \tau \beta_j^{[ks]}\right)^{1/2}}, \quad k = 1, K.$$

- 3) All users synchronously transmit their uplink signals $x^{[kj]}$, $k = 1, K$, $j = 1, L$.
- 4) All users synchronously transmit training sequences $\mathbf{r}^{[k]}$.
- 5) Base stations process received uplink signals and training sequences. In particular, each base station estimates the channel vector between itself and the users located within the same cell, and further performs decoding and precoding of uplink and downlink signals, respectively.

- 6) All base stations synchronously transmit their downlink signals $\mathbf{x}_j, j = 1, L$.

The End

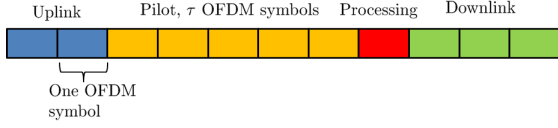


Fig. 2. Coherence block of $T = 11$ OFDM symbols

In what follows, we consider these steps in details. It is convenient to start with Step 3. **During Step 3** of the TDD protocol, the j -th base station receives uplink data signal of the form

$$\mathbf{y}_j = \sqrt{\rho_r} \sum_{k=1}^K \sum_{l=1}^L \mathbf{g}_j^{[kl]} x^{[kl]} + \mathbf{w}_j \in \mathbb{C}^{M \times 1}, \quad (2)$$

where $x^{[kl]}$ is the uplink signal of the k -th user located in the l -th cell, ρ_r is the reverse link transmit power, and $\mathbf{w}_j \sim \mathcal{CN}(0, \mathbf{I}_M)$ is the additive noise. We assume that all users have the same transmit power.

In Step 4, the j -th base station receives training signals, which can be written into a matrix $\mathbf{Y}_j \in \mathbb{C}^{M \times \tau}$ of the form

$$\mathbf{Y}_j = \sqrt{\rho_r \tau} \sum_{k=1}^K \sum_{l=1}^L \mathbf{g}_j^{[kl]} \mathbf{r}^{[k]\dagger} + \mathbf{W}_j,$$

where $\mathbf{W}_j \in \mathbb{C}^{M \times \tau}$ is the additive white Gaussian noise matrix with i.i.d. $\mathcal{CN}(0, 1)$ entries.

In Step 5, the j -th base station uses the fact that the training sequences are orthogonal to obtain the MMSE estimate of the channel vectors $\mathbf{g}_j^{[kl]}$ as (see for example [18, Chapter 12])

$$\hat{\mathbf{g}}_j^{[kj]} = \mathbf{Y}_j \left(\theta_j^{[kj]} \mathbf{r}^{[k]} \right) = \theta_j^{[kj]} \sum_{s=1}^L \sqrt{\rho_r \tau} \mathbf{g}_j^{[ks]} + \hat{\mathbf{w}}_j^{[kj]}. \quad (3)$$

where

$$\theta_j^{[kj]} = \frac{\sqrt{\rho_r \tau} \beta_j^{[kj]}}{1 + \sum_{s=1}^L \rho_r \tau \beta_j^{[ks]}}, \text{ and } \hat{\mathbf{w}}_j \sim \mathcal{CN}(0, \theta_j^{[kj]2} \mathbf{I}_M).$$

According to our Network Assumptions, base station have access to $\beta_j^{[ks]}$ and therefore are capable of finding $\hat{\mathbf{g}}_j^{[kj]}$.

Note that the vector $\hat{\mathbf{g}}_j^{[kj]}$ has the distribution

$$\hat{\mathbf{g}}_j^{[kj]} \sim \mathcal{CN} \left(0, \frac{\rho_r \tau \beta_j^{[kj]2}}{1 + \sum_{s=1}^L \rho_r \tau \beta_j^{[ks]}} \mathbf{I}_M \right). \quad (4)$$

Further, the j -th base station uses the estimates $\hat{\mathbf{g}}_j^{[kj]}$ for decoding the transmitted uplink signals $x^{[kj]}, k = 1, K$, and forming precoding beamforming vectors for downlink transmission. The decoding and precoding can be implemented in several possible ways, e.g., zero-forcing, MMSE, or matched filtering. In this work we always assume that the base station uses matched filtering for decoding and conjugate precoding

for downlink transmission. Thus, it gets an estimate of the uplink signal $x^{[kj]}$ as

$$\begin{aligned} \hat{x}^{[kj]} &= \hat{\mathbf{g}}_j^{[kj]\dagger} \mathbf{y}_j \\ &= \sqrt{\rho_r} \hat{\mathbf{g}}_j^{[kj]\dagger} \mathbf{g}_j^{[kj]} x^{[kj]} + \sum_{\substack{n=1 \\ n \neq k}}^K \sqrt{\rho_r} \hat{\mathbf{g}}_j^{[kj]} \mathbf{g}_j^{[nj]} x^{[nj]} \\ &\quad + \sum_{\substack{l=1 \\ l \neq j}}^L \sum_{n=1}^K \sqrt{\rho_r} \hat{\mathbf{g}}_j^{[kj]\dagger} \mathbf{g}_j^{[nl]} x^{[nl]} + \hat{\mathbf{g}}_j^{[kj]\dagger} \mathbf{w}^{[kj]}. \end{aligned} \quad (5)$$

For the downlink transmission, the j -th base station forms conjugate precoding beamforming vectors as

$$\mathbf{u}_j^{[k]} = \frac{\hat{\mathbf{g}}_j^{[kj]\dagger}}{\lambda_j^{[kj]}}, \quad k = 1, K, \quad (6)$$

where $\lambda_j^{[kj]2} = \mathbb{E}[\|\hat{\mathbf{g}}_j^{[kj]}\|^2]$ is the normalization factor, which according to (4), is equal to

$$\lambda_j^{[kj]2} = M \cdot \frac{\rho_r \tau \beta_j^{[kj]2}}{1 + \sum_{s=1}^L \rho_r \tau \beta_j^{[ks]}}. \quad (7)$$

The j -th base station next forms the M -dimensional vector

$$\mathbf{x}_j = \sqrt{\rho_f} \sum_{k=1}^K \mathbf{u}_j^{[k]} s^{[kj]},$$

where $s^{[kj]}$ is the downlink data signal intended for the k -th user located in the j -th cell, and ρ_f denotes forward link transmit power used by the j -th base station. We assume that all base stations use the same transmit power.

Finally, in Step 6, the j -th base station transmits and from its M antennas the vector \mathbf{x}_j .

The k -th mobile in the j -th cell receives the signal

$$\begin{aligned} y^{[kj]} &= \sum_{l=1}^L \sqrt{\rho_f} \mathbf{x}_l \mathbf{g}_l^{[kj]} + w^{[kj]} \\ &= \sqrt{\rho_f} \frac{\hat{\mathbf{g}}_j^{[kj]\dagger}}{\lambda_j^{[kj]}} \mathbf{g}_j^{[kj]} s^{[kj]} + \sum_{\substack{n=1 \\ n \neq k}}^K \sqrt{\rho_f} \frac{\hat{\mathbf{g}}_j^{[nj]\dagger}}{\lambda_j^{[nj]}} s^{[nj]} \mathbf{g}_j^{[kj]} \\ &\quad + \sum_{\substack{l=1 \\ l \neq j}}^L \sum_{n=1}^K \sqrt{\rho_f} \frac{\hat{\mathbf{g}}_l^{[nl]\dagger}}{\lambda_l^{[nl]}} s^{[nl]} \mathbf{g}_l^{[kj]} + w^{[kj]}. \end{aligned} \quad (8)$$

Note that the *effective channel* $\frac{\hat{\mathbf{g}}_j^{[kj]\dagger}}{\lambda_j^{[kj]}} \mathbf{g}_j^{[kj]}$, in average, has zero phase. The quantity

$$\epsilon_j^{[kj]} = \mathbb{E} \left[\frac{\hat{\mathbf{g}}_j^{[kj]\dagger}}{\lambda_j^{[kj]}} \mathbf{g}_j^{[kj]} \right] = \frac{\sqrt{M \rho_f \rho_r \tau} \beta_j^{[kj]}}{(1 + \sum_{s=1}^L \rho_r \tau \beta_j^{[ks]})^{1/2}}, \quad k = 1, K,$$

which the j -th base station transmits to k -th user tells the user the expected value of the power of the effective channel. So the user can use the following simple detector

$$\hat{s}^{[kj]} = \frac{y^{[kj]}}{\sqrt{\rho_f} \epsilon_j^{[kj]}}$$

for estimating the signal $s^{[kj]}$. Alternatively, instead of transmitting $\epsilon_j^{[kj]}$ at step 4 of the TDD protocol, base stations can send downlink training sequences that would allow users to estimate their effective channels. We do not elaborate on these possible details of the TDD protocol.

Note also, Steps 1 and 2 should be conducted only one time during each large-scale coherence block. As we noted in Section II-A, we do not take into account the resources needed for this.

III. LARGE-SCALE FADING PRECODING AND INTERFERENCE FREE LSAS

A. Pilot Contamination

From (5) and (8) it follows that the uplink and downlink SINRs can be written in the form presented at the top of the next page

In [3] and [10],[11] the authors considered LSASs in the asymptotic regime when the number of base station antennas M tends to infinity. The following results were obtain.

Theorem 1: The downlink SINR of the k -th terminal in the j -th cell for precoding (6) converges to the following limit:

$$\lim_{M \rightarrow \infty} \text{SINR}_D^{[kj]} \stackrel{\text{a.s.}}{=} \frac{\beta_j^{[kj]^2} / \eta_j^{[k]^2}}{\sum_{l=1, l \neq j}^L \beta_l^{[kj]^2} / \eta_l^{[k]^2}}, \quad (9)$$

where

$$\eta_l^{[k]} = \left(1 + \sum_{s=1}^L \rho_r \tau \beta_l^{[ks]} \right)^{1/2}.$$

To give an intuitive explanation of this result we remind that according to the strong law of large numbers we have the following lemma.

Lemma 2: Let $\mathbf{x}, \mathbf{y} \in \mathbb{C}^{M \times 1}$ be two independent vectors with distribution $\mathcal{CN}(\mathbf{0}, \nu \mathbf{I}_M)$. Then

$$\lim_{M \rightarrow \infty} \frac{\mathbf{x}^\dagger \mathbf{x}}{M} \stackrel{\text{a.s.}}{=} \nu \text{ and } \lim_{M \rightarrow \infty} \frac{\mathbf{x}^\dagger \mathbf{y}}{M} \stackrel{\text{a.s.}}{=} 0. \quad (10)$$

The signal $\mathbf{y}^{[kj]}$ received by the k -th user in the j -th cell is defined in (8) and estimates $\hat{\mathbf{g}}_l^{[nl]}$ are defined in (3). It is easy to see that all terms of $\hat{\mathbf{g}}_l^{[nl]}$, $n \neq k$, are independent from $\mathbf{g}_l^{[kj]}$ and therefore, according to Lemma 2 we have

$$\lim_{M \rightarrow \infty} \frac{1}{M} \hat{\mathbf{g}}_l^{[nl]\dagger} \mathbf{g}_l^{[kj]} \stackrel{\text{a.s.}}{=} 0.$$

Hence the contribution into interference of the product $\hat{\mathbf{g}}_l^{[nl]\dagger} \mathbf{g}_l^{[kj]}$ vanishes as M grows. At the same time the estimate $\hat{\mathbf{g}}_l^{[kl]\dagger}$ contains $\mathbf{g}_l^{[kj]}$ as a term. The reason for this is that the k -th users in cells j and l are using the same training sequence $\mathbf{r}^{[k]}$. Thus the product

$$\frac{1}{M} \hat{\mathbf{g}}_l^{[kl]\dagger} \mathbf{g}_l^{[kj]}$$

almost surely converges to some finite value and therefore it makes re vanishing contribution to the interference. This effect is called *pilot contamination*. It is shown in [3] and [10],[11] that pilot contamination is the only source of interference in the regime of infinitely large M .

Similar analysis of the uplink transmission leads to the following result.

Theorem 3: The uplink SINR of the k -th terminal in the j -th cell for decoding (5) converges to the following limit:

$$\lim_{M \rightarrow \infty} \text{SINR}_U^{[kj]} \stackrel{\text{a.s.}}{=} \frac{\beta_j^{[kj]^2}}{\sum_{l=1, l \neq j}^L \beta_l^{[kl]^2}}. \quad (11)$$

The natural question is whether one can mitigate the pilot contamination and further increase SINRs beyond results obtained in Theorems 1 and 3. Below we briefly discuss some approaches for this.

One possibility is to use frequency reuse for avoiding interference between adjacent cells [3]. Though the frequency reuse reduces the bandwidth, overall it allows increasing SINRs for most of the users.

Another possibility is to optimize transmit powers. In this case, the j -th base station uses the power $\rho_f^{[kj]}$ for transmitting to the k -th user in the j -th cell and transmits the vector

$$\mathbf{x}_j = \sum_{k=1}^K \sqrt{\rho_f^{[kj]}} \mathbf{u}_j^{[k]} s^{[kj]}.$$

Similarly, in the uplink transmission, the k -th user in the j -th cell will use the transmit power $\rho_r^{[kj]}$. Then, the SINR expressions (9) and (11) will be respectively

$$\lim_{M \rightarrow \infty} \text{SINR}_D^{[kj]} \stackrel{\text{a.s.}}{=} \frac{\rho_f^{[kj]} \beta_j^{[kj]^2} / \eta_j^{[k]^2}}{\sum_{l=1, l \neq j}^L \rho_f^{[kl]} \beta_l^{[kj]^2} / \eta_l^{[k]^2}}, \text{ and}$$

$$\lim_{M \rightarrow \infty} \text{SINR}_U^{[kj]} \stackrel{\text{a.s.}}{=} \frac{\rho_r^{[kj]} \beta_j^{[kj]^2}}{\sum_{l=1, l \neq j}^L \rho_r^{[kl]} \beta_l^{[kl]^2}}.$$

It is also possible to use modified TDD protocol in which users from different cells transmit pilot sequences asynchronously according to the time-shifted protocol proposed in [12],[10],[11]. For sufficiently large M the time-shifted protocol gives significant increase in downlink and uplink SINRs.

One more possibility is to replace conjugate precoding (6) with another linear precoding that mitigates the pilot contamination effect [19].

In all the above techniques, however, downlink and uplink SINRs approach some finite limits as M tends to infinity. In other words, SINRs do not grow with M .

To obtain SINRs that grow along with M , one may try to use the network MIMO approach (see for example [20],[21],[22] and references within). The network MIMO assumes that the j -th base station estimates the coefficients $\beta_j^{[kl]}$ and $h_{mj}^{[kl]}$ for all $k = 1, K$ and $l = 1, L$, and sends them to other base stations. After that, all base station start to behave as one super large antenna array. This approach, however, seems to be infeasible for the following reasons.

First, the number of small-scale fading coefficients $h_{mj}^{[kl]}$ is proportional to M . Thus, in the asymptotic regime, as M tends to infinity, the needed traffic between base stations also infinitely grows and the network MIMO becomes infeasible.

Even in the case of a finite M the needed traffic is tremendously large. Indeed, the small-scale fading coefficients

$$\text{SINR}_U^{[kj]} = \frac{\rho_r |\hat{\mathbf{g}}_j^{[kj]\dagger} \mathbf{g}_j^{[kj]}|^2}{\sum_{\substack{n=1 \\ n \neq k}}^K \rho_r |\hat{\mathbf{g}}_j^{[kj]} \mathbf{g}_j^{[nj]}|^2 + \sum_{\substack{l=1 \\ l \neq j}}^L \sum_{n=1}^K \rho_r |\hat{\mathbf{g}}_j^{[kj]\dagger} \mathbf{g}_j^{[nl]}|^2 + \text{Var}[\hat{\mathbf{g}}_j^{[kj]\dagger} w^{[kj]}]}$$

$$\text{SINR}_D^{[kj]} = \frac{\frac{\rho_f}{\lambda_j^{[kj]}} |\hat{\mathbf{g}}_j^{[kj]\dagger} \mathbf{g}_j^{[kj]}|^2}{\sum_{\substack{n=1 \\ n \neq k}}^K \frac{\rho_f}{\lambda_j^{[nj]}} |\hat{\mathbf{g}}_j^{[nj]\dagger} \mathbf{g}_j^{[kj]}|^2 + \sum_{\substack{l=1 \\ l \neq j}}^L \sum_{n=1}^K \frac{\rho_f}{\lambda_l^{[nl]}} |\hat{\mathbf{g}}_l^{[nl]\dagger} \mathbf{g}_l^{[kj]}|^2 + \text{Var}[w^{[kj]}]}$$

depend on frequency. The typical assumption is that small-scale fading coefficients $h_{m_j}^{[kl]}$ of OFDM tones i and $i + \Delta$ are considered being independent random variables when Δ is the coherent bandwidth, which typically is in between 10 and 20 subcarriers.. Thus, if $M = 100$ and the total number of OFDM subcarriers is say $N = 1400$, and $\Delta = 14$, then the j -th base station needs to transmit to other base stations $NM/\Delta \cdot K(L - 1) = 10000K(L - 1)$ small-scale fading coefficients for given k and l . Note that the small-scale fading coefficients substantially change as soon as a mobile moves a quarter of the wavelength. Taking all this into account we conclude that the needed traffic between base stations is hardly feasible.

The second reason is even more fundamental. Since users in different cells reuse the same pilot sequences, the j -th base station is not capable of obtaining independent estimates for the coefficients $h_{m_j}^{[kj]}$ and $h_{m_j}^{[kl]}$, since the k -th users in cells j and l use the same pilot sequence $\mathbf{r}^{[k]}$. Thus, the standard network MIMO approach is not applicable even if we ignore the traffic problem.

One possible conclusion of the above arguments can be that in both noncooperative LSASs and LSASs with cooperation (like network MIMO), SINRs do not grow with M beyond certain limits. In this paper, we disprove the above statement. We demonstrate that limited cooperation between base stations allows us to completely resolve the pilot contamination problem and to construct interference and noise free LSASs with infinite downlink and uplink SINRs.

B. Large-Scale Fading Precoding

We start with changing the Network Assumption defined in Section II.

Network Assumptions II

- 1) We assume that the j -th base station can accurately estimate and track large-scale fading coefficients $\beta_j^{[kl]}$, $k = 1, K$ and $l = 1, L$.
- 2) If $\epsilon_j^{[kj]}$ is a quantity that depends only on large-scale fading coefficients we assume that the j -th base station can forward it to the k -th user in the j -th cell.
- 3) We assume that all base stations are connected to a network controller (as it is shown in Fig. 3) and that the large-scale fading coefficients $\beta_j^{[kl]}$ are accessible to the network controller.
- 4) We assume that all downlink signals $s^{[kj]}$ with $j = 1, L$, $k = 1, K$, are accessible to all base stations.

Remark 1: We assume that the network controller and base stations have access to all, across the entire network, $\beta_j^{[kl]}$ and

$s^{[kj]}$ respectively, only in order to obtain a simple theoretical model. In Part II of the paper [2], we will replace these assumptions with more realistic ones.

Remark 2: We would like to point out that the large-scale fading coefficients $\beta_j^{[kl]}$ are relatively easy to estimate and track. One possible approach for this is outlined at the end of this section.

Below we describe the *Large-Scale Fading Precoding* protocol for interference mitigation in LSASs. Originally we designed this protocol in cite [15] and [16] for canceling the directed interference caused by pilot contamination and called it *Pilot Contamination Precoding* (PCP). Recently, however, we came to the conclusion that that the name Large-Scale Fading Precoding better reflects the idea of this protocol.

Large-Scale Fading Precoding (LSFP)

- 1) In the beginning of each large-scale coherence block (of duration T_β OFDM symbols) the j -th base station estimates the large-scale fading coefficients $\beta_j^{[kl]}$, $k = 1, K$, $l = 1, L$, and sends them to the network controller.
- 2) The network controller computes the $L \times L$ LSFP precoding matrices

$$\Phi^{[k]} = \begin{pmatrix} \frac{\phi_1^{[k]}}{\lambda_1^{[k]}} \\ \frac{\phi_2^{[k]}}{\lambda_2^{[k]}} \\ \vdots \\ \frac{\phi_L^{[k]}}{\lambda_L^{[k]}} \end{pmatrix}, \quad k = 1, K,$$

as functions of $\beta_j^{[kl]}$, $j, l = 1, \dots, L$, so that

$$\|\underline{\phi}_l^{[k]}\|^2 \leq 1, \quad (12)$$

and sends the rows $\underline{\phi}_j^{[k]}$, $k = 1, K$, to the j -th base station.

- 3) The network controller computes quantities

$$\epsilon_j^{[kj]} = \sqrt{\rho_f} M \rho_r \tau \sum_{l=1}^L \frac{\beta_l^{[kj]} \beta_l^{[kl]}}{1 + \sum_{s=1}^L \rho_r \tau \beta_l^{[ks]} \lambda_l^{[kl]}} \frac{\phi_l^{[kj]}}{\lambda_l^{[kl]}}, \quad k = 1, K,$$

(where $\phi_j^{[kl]}$ is the (j, l) entry of $\Phi^{[k]}$) and sends them to the j -th base station, which sends them further to the corresponding users located in the j -th cell.

- 4) The j -th base station conducts **large-scale fading pre-**

coding. Namely, it computes signals

$$c_j^{[k]} = \phi_j^{[k]} \begin{pmatrix} s^{[k1]} \\ s^{[k2]} \\ \vdots \\ s^{[kL]} \end{pmatrix}, \quad k = 1, K. \quad (13)$$

(Since $\text{Var}[s^{[kj]}] = 1$, the constraint (12) implies that $\text{Var}[c_j^{[k]}] = 1$.)

- 5) The j -th base station obtains the MMSE estimates $\hat{\mathbf{g}}_j^{[kj]}$, $k = 1, K$, according to (3).
- 6) The j -th base station performs **small-scale fading precoding**, namely it forms conjugate precoding beamforming vectors

$$\mathbf{u}_j^{[k]} = \frac{\hat{\mathbf{g}}_j^{[kj]\dagger}}{\lambda_j^{[kj]}}, \quad k = 1, K,$$

and transmits from its M antennas the vector

$$\mathbf{x}_j = \sqrt{\rho_f} \sum_{k=1}^K \mathbf{u}_j^{[k]} c_j^{[k]}.$$

(Note that other types of small-scale precodings can be used at this step. For instance, vectors $\mathbf{u}_j^{[k]}$ can be formed with the help of M -dimensional zero-forcing precoding.)

The End

The block diagram of this protocol is shown in Fig.3.

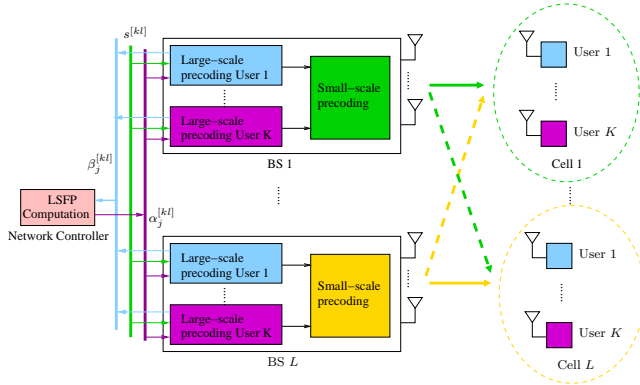


Fig. 3. System diagram for the LSFP. Each BS performs two levels of precoding. Multi-cell cooperation is based on the large-scale fading coefficients only. Each BS also performs local precoding using estimates of M -dimensional fast fading vectors.

We would like to point out the following things about this algorithm.

- No exchange of small-scale fading coefficients $h_{m,j}^{[kl]}$ between base stations and the network controller is required (opposite to the network MIMO).
- Steps 1 – 3 are conducted once every large-scale coherence block, which is typically about 40 times longer than the coherence blocks of small-scale coefficients.
- The purpose of quantities $\epsilon_j^{[kj]}$ is to send to the corresponding users the expected powers of their effective channels (see (33) and (34) in Section IV for details). If

the k -th user in the j -th cell receives the signal $y^{[kj]}$ it can estimate the signal $s^{[kj]}$ as

$$\hat{s}^{[kj]} = \frac{y^{[kj]}}{\epsilon_j^{[kj]}}.$$

Alternatively, instead of sending $\epsilon_j^{[kj]}$ base stations can send downlink training sequences.

- The estimates $\hat{\mathbf{g}}_j^{[kl]}$ are computed one time for each coherence block of small-scale coefficients, that is once every T OFDM symbols.
- The quantity $c_j^{[k]}$ and vector \mathbf{x}_j are computed for each channel use (each downlink OFDM symbol).

Now we show that an appropriate choice of LSFP precoding matrices $\Phi^{[k]}$ allows one to completely cancel the interference and noise as M tends to infinity. Let us define $L \times L$ matrices composed of large scale fading coefficients

$$\mathbf{B}_D^{[k]} = \begin{pmatrix} \beta_1^{[k1]}/\eta_1^{[k]} & \dots & \beta_L^{[k1]}/\eta_L^{[k]} \\ \vdots & & \vdots \\ \beta_1^{[kL]}/\eta_1^{[k]} & \dots & \beta_L^{[kL]}/\eta_L^{[k]} \end{pmatrix}. \quad (14)$$

For $B_D^{[k]}$ of full rank we define *Zero-Forcing LSFP* (ZF-LSFP) as the above LSFP with

$$\Phi^{[k]} = \sqrt{\rho_A} \mathbf{B}_D^{[k]-1}, \quad k = 1, K, \quad (15)$$

where ρ_A is a normalization factor to insure the constraint (12).

For analysis of ZF-LSFP it is convenient to make a small modification of the LSFP assuming that at Step 3 $\epsilon_j^{[kj]} = \sqrt{M} \rho_f \rho_r \rho_A \tau$.

Let us assume now that signals $s^{[kj]}$ are taken from a signal constellation $\mathcal{R} = \{r_1, \dots, r_N\}$ according to some probability mass function (PMF) $P_S(\cdot)$. Define further the entropy

$$H(s^{[kj]}) = - \sum_{s \in \mathcal{R}} P_S(s) \log P_S(s).$$

Assume also that all $|r_j|, r_j \in \mathcal{R}$, are finite.

The k -th user in the j -th cell receives the signal

$$y^{[kj]} = \sum_{l=1}^L \sum_{n=1}^K \frac{\sqrt{\rho_f}}{\lambda_l^{[nl]}} \hat{\mathbf{g}}_l^{[nl]\dagger} \mathbf{g}_l^{[nj]} c_l^{[n]} + w^{[kj]}. \quad (16)$$

Let the user uses the following simple detection method of the transmitted signal $s^{[kj]}$:

$$\hat{s}_M^{[kj]} = \frac{y^{[kj]}}{\sqrt{M} \rho_f \rho_r \rho_A \tau}. \quad (17)$$

The following theorem shows that in the asymptotic regime, as $M \rightarrow \infty$, the ZF-LSFP allows one to reliably transmit signals from an arbitrary large \mathcal{R} and therefore it provides infinite capacity.

Theorem 4: For ZF-LSFP we have

$$\lim_{M \rightarrow \infty} I(\hat{s}_M^{[kj]}; s^{[kj]}) = H(s^{[kj]}), \quad k = 1, K, \quad j = 1, L. \quad (18)$$

To prove this theorem we need the following lemma. Let

$$s_M = a_M \cdot s + w_M,$$

where s is a random signal from \mathcal{R} and a_M and w_M are random variables (not necessarily independent) such that

$$\lim_{M \rightarrow \infty} a_M \stackrel{\text{a.s.}}{=} 1 \text{ and } \lim_{M \rightarrow \infty} w_M \stackrel{\text{a.s.}}{=} 0. \quad (19)$$

Lemma 5:

$$\lim_{M \rightarrow \infty} I(s_M; s) = H(s).$$

A proof of this lemma is in Appendix A.

We will also need the following well known fact. Let ϕ and β be some constants and a_M and b_M be random variables so that

$$\lim_{M \rightarrow \infty} a_M \stackrel{\text{a.s.}}{=} a \text{ and } \lim_{M \rightarrow \infty} w_M \stackrel{\text{a.s.}}{=} b,$$

where a and b are some constants. Then

$$\lim_{M \rightarrow \infty} a_M \phi + b_M \beta \stackrel{\text{a.s.}}{=} a\phi + b\beta. \quad (20)$$

Indeed, let (Ω, \mathcal{F}, P) be the probability space on which a_M and b_M are defined. Let further

$$\mathcal{A} = \{\omega \in \Omega : \lim_{M \rightarrow \infty} a_M(\omega) = a\},$$

$$\mathcal{B} = \{\omega \in \Omega : \lim_{M \rightarrow \infty} b_M(\omega) = b\}, \text{ and}$$

$$\mathcal{C} = \{\omega \in \Omega : \lim_{M \rightarrow \infty} a_m(\omega)\phi + b_m(\omega)\beta = a\phi + b\beta\}.$$

Then $\mathcal{A} \cap \mathcal{B} \subseteq \mathcal{C}$. So we have

$$\begin{aligned} \Pr(\mathcal{C}) &\geq \Pr(\mathcal{A} \cap \mathcal{B}) = \Pr((\mathcal{A}^c \cup \mathcal{B}^c)^c) \\ &= 1 - \Pr(\mathcal{A}^c \cup \mathcal{B}^c) \geq 1 - \Pr(\mathcal{A}^c) - \Pr(\mathcal{B}^c) = 1. \end{aligned}$$

Proof: (Theorem 4) The signal $y^{[kj]}$ defined in (16) can be written in the form:

$$\begin{aligned} &y^{[kj]} \\ &= \sum_{l=1}^L \frac{\sqrt{\rho_f}}{\lambda_l^{[kl]}} \hat{\mathbf{g}}_l^{[kl]\dagger} \mathbf{g}_l^{[kj]} c_l^{[k]} + \sum_{l=1}^L \sum_{\substack{n=1 \\ n \neq k}}^K \frac{\sqrt{\rho_f}}{\lambda_l^{[nl]}} \hat{\mathbf{g}}_l^{[nl]\dagger} \mathbf{g}_l^{[kj]} c_l^{[n]} + w^{[kj]}, \end{aligned} \quad (21)$$

Let us denote the factors in front of $c_l^{[k]}$ in the first sum by

$$\begin{aligned} f_l^{[kj]} &= \frac{\sqrt{\rho_f}}{\lambda_l^{[kl]}} \hat{\mathbf{g}}_l^{[kl]\dagger} \mathbf{g}_l^{[kj]} \\ &= \frac{\sqrt{\rho_f}}{\lambda_l^{[kl]}} \theta_l^{[kl]} \left(\sum_{s=1}^L \sqrt{\rho_r \tau} \mathbf{g}_l^{[ks]\dagger} + \hat{\mathbf{w}}_l^{[kl]\dagger} \right) \mathbf{g}_l^{[kj]}. \end{aligned}$$

Opening the parenthesis and applying Lemma 2 to each term of the above expression, we obtain

$$\lim_{M \rightarrow \infty} \frac{1}{\sqrt{M}} f_l^{[kj]} \stackrel{\text{a.s.}}{=} \frac{\sqrt{\rho_f \rho_r \tau}}{\eta_l^{[k]}} \beta_l^{[kj]}. \quad (22)$$

Denote further the terms in the second sum of (21) by

$$\begin{aligned} q_{nl}^{[kj]} &= \frac{\sqrt{\rho_f}}{\lambda_l^{[nl]}} \hat{\mathbf{g}}_l^{[nl]\dagger} \mathbf{g}_l^{[kj]} c_l^{[n]} \\ &= \frac{\sqrt{\rho_f}}{\lambda_l^{[nl]}} \theta_l^{[nl]} \left(\sum_{s=1}^L \sqrt{\rho_r \tau} \mathbf{g}_l^{[ns]\dagger} + \hat{\mathbf{w}}_l^{[nl]\dagger} \right) \mathbf{g}_l^{[kj]} c_l^{[n]} \end{aligned}$$

Again, using Lemma 2, we obtain

$$\lim_{M \rightarrow \infty} \frac{1}{\sqrt{M}} q_{nl}^{[kj]} \stackrel{\text{a.s.}}{=} 0. \quad (23)$$

For $k = 1, K$, denote

$$F^{[k]} = \begin{pmatrix} f_1^{[k1]} & \dots & f_L^{[k1]} \\ \vdots & & \vdots \\ f_1^{[kL]} & \dots & f_L^{[kL]} \end{pmatrix},$$

and

$$\mathbf{y}^{[k]} = \begin{pmatrix} y^{[k1]} \\ \vdots \\ y^{[kL]} \end{pmatrix}, \mathbf{c}^{[k]} = \begin{pmatrix} c_1^{[k]} \\ \vdots \\ c_L^{[k]} \end{pmatrix}, \mathbf{s}^{[k]} = \begin{pmatrix} s^{[k1]} \\ \vdots \\ s^{[kL]} \end{pmatrix},$$

and

$$\mathbf{q}^{[k]} = \begin{pmatrix} \sum_{l=1}^L \sum_{\substack{n=1 \\ n \neq k}}^K q_{nl}^{[k1]} \\ \vdots \\ \sum_{l=1}^L \sum_{\substack{n=1 \\ n \neq k}}^K q_{nl}^{[kL]} \end{pmatrix}, \mathbf{w}^{[k]} = \begin{pmatrix} w^{[k1]} \\ \vdots \\ w^{[kL]} \end{pmatrix}.$$

With this notations we have

$$\mathbf{y}^{[k]} = F^{[k]} \mathbf{c}^{[k]} + \mathbf{q}^{[k]} + \mathbf{w}^{[k]} = F^{[k]} \Phi^{[k]} \mathbf{s}^{[k]} + \mathbf{q}^{[k]} + \mathbf{w}^{[k]}. \quad (24)$$

Let $V^{[k]} = F^{[k]} \Phi^{[k]}$. According to (22) we have that the entries of $F^{[k]}$ almost surely converge to the corresponding entries of the matrix $\sqrt{\rho_f \rho_r \tau} B_D^{[k]}$. From this, (20), and from the definition of $\Phi^{[k]}$ it follows that the entries $v_{im}^{[k]}$ of $V^{[k]}$ have the property:

$$\lim_{M \rightarrow \infty} \frac{1}{\sqrt{M}} v_{im}^{[k]} \stackrel{\text{a.s.}}{=} \delta_{im} \sqrt{\rho_f \rho_r \rho_A \tau}, \quad i, m = 1, L.$$

From (24) and (17) we have

$$\begin{aligned} \hat{s}_M^{[kj]} &= \frac{1}{\sqrt{M}} \frac{1}{\sqrt{\rho_f \rho_r \rho_A \tau}} (v_{jj}^{[k]} s^{[kj]} + \sum_{l \neq j} v_{jl}^{[k]} s^{[kl]} \\ &\quad + \sum_{l=1}^L \sum_{\substack{n=1 \\ n \neq k}}^K q_{nl}^{[kj]} + w^{[kj]}). \end{aligned}$$

Applying now Lemma 5 to the above expression we obtain

$$\lim_{M \rightarrow \infty} I(\hat{s}_M^{[kj]}; s^{[kj]}) = H(s^{[kj]}). \quad \blacksquare$$

Thus, under our network assumptions defined in Section III, we constructed a noise free and interference free multi-cell LSAS with frequency reuse 1. In such LSAS the size of modulation \mathcal{R} can be chosen arbitrary large and therefore the LSAS can achieve an arbitrary large capacity.

C. Large-Scale Fading Decoding

With the same Network Assumptions II we define the following protocol for uplink data transmission.

Large-Scale Fading Decoding

- 1) The j -th base station estimates the large scale fading coefficients $\beta_j^{[kn]}$, $k = 1, K$, $n = 1, L$, and sends them to the network controller.

2) The controller computes $L \times L$ decoding matrices

$$\Omega^{[k]} = \begin{pmatrix} \underline{\omega}_1^{[k]} \\ \underline{\omega}_2^{[k]} \\ \vdots \\ \underline{\omega}_L^{[k]} \end{pmatrix}, \quad k = 1, K,$$

as functions of $\beta_j^{[kl]}$, $j, l = 1, L$.

3) The j -th base station computes the MMSE estimates $\hat{\mathbf{g}}_j^{[kj]}$, $k = 1, \dots, K$ according to (3).

4) The j -th base station receives the vector \mathbf{y}_j defined in (2) and computes the matched filtering estimates

$$\hat{x}^{[kj]} = \hat{\mathbf{g}}_j^{[kj]\dagger} \mathbf{y}_j, \quad k = 1, \dots, K,$$

of the uplink signals $x^{[kj]}$ (other options, for instance M -dimensional Zero Forcing or MMSE receiver, are possible here) and sends them to the network controller.

5) The network controller computes the following estimates of $x^{[kj]}$

$$\hat{x}_M^{[kj]} = \frac{1}{M\theta_j^{[kj]}\rho_r\sqrt{\tau}}\omega_j^{[k]} \begin{pmatrix} \tilde{x}^{[k1]} \\ \vdots \\ \tilde{x}^{[kL]} \end{pmatrix}, \quad k = 1, \dots, K.$$

The End

We would like to point out the following things.

- Unlike the network MIMO approach, small-scale fading coefficients $h_{mj}^{[kj]}$ are used locally by the j -th base station and are not sent to the network controller.
- Steps 1 and 2 are conducted only one time every large-scale coherence block, that is once every T_β OFDM symbols.
- The estimates $\hat{\mathbf{g}}_j^{[kj]}$ at Step 3 are computed one time for each coherence block, that is once every T OFDM symbols.
- Step 4 and 5 are conducted for each channel use (each OFDM symbol).

Let

$$\mathbf{B}_U^{[k]} = \begin{pmatrix} \beta_1^{[k1]} & \dots & \beta_1^{[kL]} \\ \vdots & & \vdots \\ \beta_L^{[k1]} & \dots & \beta_L^{[kL]} \end{pmatrix}.$$

Similar to the downlink case, we define *Zero-Forcing LSFD* as LSFD with

$$\Omega^{[k]} = \mathbf{B}_U^{[k]-1}, \quad k = 1, K. \quad (25)$$

We again assume that signals $x^{[kj]}$ belong to a signal constellation $\mathcal{R} = \{r_1, \dots, r_N\}$ with PMF $P_S(\cdot)$.

Theorem 6: For Large-Scale Fading Decoding, we have

$$\lim_{M \rightarrow \infty} I(\hat{x}_M^{[kj]}; x^{[kj]}) = H(x^{[kj]}).$$

Proof: Using (2) and (3), we get

$$\begin{aligned} \tilde{x}^{[kj]} &= \hat{\mathbf{g}}_j^{[kj]\dagger} \mathbf{y}_j \\ &= \sum_{l=1}^L x^{[kl]} \theta_j^{[kj]} \underbrace{\sum_{s=1}^L \rho_r \sqrt{\tau} \mathbf{g}_j^{[ks]\dagger} \mathbf{g}_j^{[kl]}}_{f_j^{[kl]}} \\ &\quad + \underbrace{\theta_j^{[kj]} \sum_{s=1}^L (\sqrt{\rho_r \tau} \mathbf{g}_j^{[ks]} + \hat{\mathbf{w}}_j^{[kj]})^\dagger \left(\sum_{l=1}^L \sum_{\substack{n=1 \\ n \neq k}}^K \sqrt{\rho_r} \mathbf{g}_j^{[nl]} x^{[nl]} + \mathbf{w}_j \right)}_{q^{[kj]}} \end{aligned}$$

Applying Lemma 1 we obtain

$$\begin{aligned} \lim_{M \rightarrow \infty} \frac{1}{M} f_j^{[kl]} &\stackrel{\text{a.s.}}{=} \theta_j^{[kj]} \rho_r \sqrt{\tau} \beta_j^{[kl]}, \quad \text{and} \\ \lim_{M \rightarrow \infty} \frac{1}{M} q^{[kj]} &\stackrel{\text{a.s.}}{=} 0. \end{aligned}$$

Denote

$$F^{[k]} = \begin{pmatrix} f_1^{[k1]} & \dots & f_1^{[kL]} \\ \vdots & & \vdots \\ f_L^{[k1]} & \dots & f_L^{[kL]} \end{pmatrix},$$

and

$$\tilde{\mathbf{x}}^{[k]} = \begin{pmatrix} \tilde{x}^{[k1]} \\ \vdots \\ \tilde{x}^{[kL]} \end{pmatrix}, \quad \mathbf{x}^{[k]} = \begin{pmatrix} x^{[k1]} \\ \vdots \\ x^{[kL]} \end{pmatrix}, \quad \mathbf{q}^{[k]} = \begin{pmatrix} q^{[k1]} \\ \vdots \\ q^{[kL]} \end{pmatrix}.$$

We this notations we have

$$\tilde{\mathbf{x}}^{[k]} = F^{[k]} \mathbf{x}^{[k]} + \mathbf{q}^{[k]}.$$

Hence

$$\begin{aligned} \begin{pmatrix} \hat{x}_M^{[k1]} \\ \vdots \\ \hat{x}_M^{[kL]} \end{pmatrix} &= \frac{1}{M\theta_j^{[kj]}\rho_r\sqrt{\tau}} \Omega^{[k]} \tilde{\mathbf{x}}^{[k]} \\ &= \frac{1}{M\theta_j^{[kj]}\rho_r\sqrt{\tau}} (\Omega^{[k]} F^{[k]} \mathbf{x}^{[k]} + \Omega^{[k]} \mathbf{q}^{[k]}). \quad (26) \end{aligned}$$

Note that as M grows the matrix $F^{[k]}$ almost surely converges to the matrix $\theta_j^{[kj]} \rho_r \sqrt{\tau} B_U^{[k]}$.

Let $V^{[k]} = \Omega^{[k]} F^{[k]}$. Applying Lemma 2 and (20) to the entries of $V^{[k]}$, we get

$$\lim_{M \rightarrow \infty} \frac{1}{M\theta_j^{[kj]}\rho_r\sqrt{\tau}} v_{im}^{[k]} \stackrel{\text{a.s.}}{=} \delta_{im}, \quad i, m = 1, L.$$

From Lemma 2 and (20) it also follows that each entry of the vector $\Phi^{[k]} \mathbf{q}^{[k]}$ almost surely converges to 0. Now applying Lemma 5 to the entries of the vector (26) we obtain

$$\lim_{M \rightarrow \infty} I(\hat{x}_M^{[kj]}; x^{[kj]}) = H(x^{[kj]}).$$

Again we obtained a noise free and interference free multi-cell LSAS, that is an LSAS with arbitrary large capacity, with frequency reuse 1. ■

D. Estimation of Large-Scale Fading Coefficients

In this subsection we outline one possible algorithm for estimation of large-scale fading coefficients.

First, we would like to remind that the coefficients $\beta_j^{[kl]}$ do not depend on antenna indices as well as on OFDM tone indices. Thus, between any given base station and a mobile, there is only one large-scale fading coefficient. Second, these coefficients change only when a mobile significantly change its geographical location. The standard assumption is that in the radius of 10 wavelengths, the large-scale fading coefficients are approximately constant. In contrast, small-scale fading coefficients significantly change as soon as a user moves by a quarter of the wavelength. Thus, large-scale fading coefficients change about 40 times slower than small-scale fading coefficients.

Let us enumerate all users across the entire network by integers from 1 to LK . Denote by $\beta_j^{[i]}$ and $\mathbf{h}_j^{[i]}$ the large-scale fading coefficient and fast fading vector between the i -th users and the j -th base station. Let further $\mathbf{v}^{[r]}$, $r = 1, \mu$, be a set of mutually orthogonal μ -tuples of norm 1. Since the coefficient $\beta_j^{[i]}$ does not depend on OFDM tone indices, it is enough if the i -th user transmits a training sequence, say $\mathbf{v}^{[1]}$, in only one OFDM tone. We assume that no other user transmits $\mathbf{v}^{[1]}$ in this OFDM tones and that users that transmit $\mathbf{v}^{[r]}$, $r \geq 2$, in this OFDM tone are enumerated by $2, \dots, \mu$. In this OFDM tone the j -th base station receives the signal

$$\mathbf{Y}_j = \sqrt{\rho_r \mu} \sqrt{\beta_j^{[i]}} \mathbf{h}_j^{[i]} \mathbf{v}^{[i]\dagger} + \sum_{k=2}^{\mu} \sqrt{\rho_r \mu} \sqrt{\beta_j^{[k]}} \mathbf{h}_j^{[k]} \mathbf{v}^{[k]} + \mathbf{W}_j,$$

where $\mathbf{W}_j \in \mathbb{C}^{M \times \mu}$ is the additive white Gaussian noise matrix with i.i.d. $\mathcal{CN}(0, 1)$ entries. In order to estimate $\beta_j^{[i]}$, the j -th base station first computes

$$\mathbf{y} = \mathbf{Y}_j \mathbf{v}^{[1]} = \sqrt{\rho_r \mu} \sqrt{\beta_j^{[kl]}} \mathbf{h}_j^{[kl]} + \hat{\mathbf{w}}_j,$$

and further

$$\hat{\beta}_j^{[i]} = \frac{1}{M \rho_r \mu} \mathbf{y}^\dagger \mathbf{y} - \frac{1}{\rho_r \mu}.$$

Taking into account that $\hat{\mathbf{w}}_j \sim \mathcal{CN}(0, \mathbf{I}_M)$ and using Lemma 2, after simple computations, we obtain

$$\lim_{M \rightarrow \infty} \hat{\beta}_j^{[kl]} \stackrel{\text{a.s.}}{=} \beta_j^{[kl]}.$$

Training sequences transmitted in different OFDM tones do not interfere with each other. Thus if N is the number of OFDM tones the above approach allows us to have $N\mu$ non interfering training sequences. For example if $N = 1400$, $\mu = 8$, and $K = 20$ this approach allows one to estimate large-scale fading coefficients in a network of $L = 560$ cells. In real life application we need to estimate large-scale coefficients only of the users located in neighboring cells and users located far away from each other can reuse the same OFDM tone and training sequence.

IV. FINITE M ANALYSIS

In this section we derive SINR expressions for downlink and uplink LSFPs in which the number M of base station antennas

appears as a parameter. We do not assume ZF-LSFP, instead we consider generic LSFPs in which matrices $\Phi^{[k]}$ and $\Omega^{[k]}$ can have arbitrary entries, with the constraints that the transmit powers of each base station and each user, in average, do not exceed ρ_f and ρ_r respectively.

First, we would like to note that though the j -th base stations needs only MMSE estimates $\hat{\mathbf{g}}_j^{[kj]}$, $k = 1, K$, it can also compute the MMSE estimates of the channel vectors $\hat{\mathbf{g}}_j^{[kl]}$, $k = 1, K$, $l = 1, L$, between itself and all the users in the network as

$$\hat{\mathbf{g}}_j^{[kl]} = \mathbf{Y}_j(\theta_j^{[kl]} \mathbf{r}^{[k]}) = \theta_j^{[kl]} \sqrt{\rho_r \tau} \sum_{s=1}^L \mathbf{g}_j^{[ks]} + \hat{\mathbf{w}}_j^{[kl]}, \quad (27)$$

where

$$\theta_j^{[kl]} = \frac{\sqrt{\rho_r \tau} \beta_j^{[kl]}}{1 + \rho_r \tau \sum_{s=1}^L \beta_j^{[ks]}},$$

and $\hat{\mathbf{w}}_j^{[kl]} \sim \mathcal{CN}(0, \theta_j^{[kl]^2} \mathbf{I}_M)$. Let

$$\tilde{\mathbf{g}}_j^{[kl]} = \mathbf{g} - \hat{\mathbf{g}}_j^{[kl]}$$

be the estimation error.

The following properties of $\hat{\mathbf{g}}_j^{[kl]}$ and $\tilde{\mathbf{g}}_j^{[kl]}$ are either well known (see for example [18]) or can be easily derived from their definitions.

- 1) If $(j, k) \neq (j', k')$ then the vectors $\hat{\mathbf{g}}_j^{[kl]}$ and $\hat{\mathbf{g}}_{j'}^{[k's]}$ are independent for any l and s .
- 2) The vectors $\hat{\mathbf{g}}_j^{[kl]}$ and $\hat{\mathbf{g}}_i^{[n,s]}$ are uncorrelated for any indices j, k, l, i, n , and s .
- 3) The vectors $\hat{\mathbf{g}}_j^{[kl]}$ and $\tilde{\mathbf{g}}_j^{[kl]}$ have the following distributions:

$$\hat{\mathbf{g}}_j^{[kl]} \sim \mathcal{CN} \left(0, \frac{\rho_r \tau \beta_j^{[kl]^2}}{1 + \sum_{s=1}^L \rho_r \tau \beta_j^{[ks]}} \mathbf{I}_M \right), \quad (28)$$

and

$$\tilde{\mathbf{g}}_j^{[kl]} \sim \mathcal{CN} \left(0, \left(\beta_j^{[kl]} - \frac{\rho_r \tau \beta_j^{[kl]}}{1 + \sum_{s=1}^L \rho_r \tau \beta_j^{[ks]}} \right) \mathbf{I}_M \right). \quad (29)$$

- 4) It is not difficult to show that

$$\mathbb{E}[\hat{\mathbf{g}}_j^{[kl]} \hat{\mathbf{g}}_j^{[kj]\dagger}] = \frac{\rho_r \tau \beta_j^{[kl]} \beta_j^{[kj]}}{1 + \sum_{s=1}^L \rho_r \tau \beta_j^{[ks]}} \mathbf{I}_M. \quad (30)$$

A. Performance of Large-Scale Fading Precoding with Finite M

Denote the (j, v) entry of matrix $\Phi^{[k]}$ by $\phi_j^{[kv]}$. It will be convenient for us to assume that in LSFP protocol the normalization coefficients $\frac{1}{\lambda_j^{[kj]}}$, used in Step 6 of LSFP, are absorbed into the $\phi_j^{[kv]}$. In other words, we replace $\phi_j^{[kv]}$ with $\frac{\phi_j^{[kv]}}{\lambda_j^{[kj]}}$ and in Step 6 use $\mathbf{u}_j^{[k]} = \hat{\mathbf{g}}_j^{[kj]\dagger}$. This allows us to shorten notations.

According to the LSFP protocol, the k -th terminal in the l -th cell receives the signal

$$\begin{aligned} y^{[kl]} &= \sqrt{\rho_f} \sum_{j=1}^L \mathbf{x}_j \mathbf{g}_j^{[kl]} + w^{[kl]} \\ &= \sum_{j=1}^L \sum_{n=1}^K \hat{\mathbf{g}}_j^{[nj]\dagger} c_j^{[n]} \mathbf{g}_j^{[kl]} + w^{[kl]}. \end{aligned} \quad (31)$$

Taking into account that

$$\begin{aligned} \mathbf{g}_j^{[kl]} &= \hat{\mathbf{g}}_j^{[kl]} + \tilde{\mathbf{g}}_j^{[kl]}, \text{ and} \\ c_j^{[k]} &= \sum_{v=1}^L \phi_j^{[kv]} s^{[kv]}, \end{aligned} \quad (32)$$

and replacing the random variable in front of $s^{[kl]}$ with its expected value we obtain:

$$\begin{aligned} & y^{[kl]} \\ &= \sqrt{\rho_f} \sum_{j=1}^L \sum_{n=1}^K \hat{\mathbf{g}}_j^{[nj]\dagger} \hat{\mathbf{g}}_j^{[kl]} c_j^{[n]} + \sqrt{\rho_f} \sum_{j=1}^L \sum_{n=1}^K \hat{\mathbf{g}}_j^{[nj]\dagger} \tilde{\mathbf{g}}_j^{[kl]} c_j^{[n]} \\ & \quad + w^{[kl]} \\ &= s^{[kl]} \sqrt{\rho_f} \sum_{j=1}^L \phi_j^{[kl]} \hat{\mathbf{g}}_j^{[kj]\dagger} \hat{\mathbf{g}}_j^{[kl]} \\ & \quad + \sqrt{\rho_f} \sum_{\substack{v=1 \\ v \neq l}}^L s^{[kv]} \sum_{j=1}^L \phi_j^{[kv]} \hat{\mathbf{g}}_j^{[kj]\dagger} \hat{\mathbf{g}}_j^{[kl]} \\ & \quad + \sqrt{\rho_f} \sum_{j=1}^L \sum_{\substack{n=1 \\ n \neq k}}^K \hat{\mathbf{g}}_j^{[nj]\dagger} \hat{\mathbf{g}}_j^{[kl]} c_j^{[n]} + \sqrt{\rho_f} \sum_{j=1}^L \sum_{n=1}^K \hat{\mathbf{g}}_j^{[nj]\dagger} \tilde{\mathbf{g}}_j^{[kl]} c_j^{[n]} \\ & \quad + w^{[kl]} \\ &= \underbrace{s^{[kl]} \sqrt{\rho_f} \sum_{j=1}^L \phi_j^{[kl]} \mathbb{E}[\hat{\mathbf{g}}_j^{[kj]\dagger} \hat{\mathbf{g}}_j^{[kl]}]}_{T_0} \\ & \quad + \underbrace{\sqrt{\rho_f} s^{[kl]} \sum_{j=1}^L \phi_j^{[kl]} (\hat{\mathbf{g}}_j^{[kj]\dagger} \hat{\mathbf{g}}_j^{[kl]} - \mathbb{E}[\hat{\mathbf{g}}_j^{[kj]\dagger} \hat{\mathbf{g}}_j^{[kl]}])}_{T_1} \\ & \quad + \underbrace{\sqrt{\rho_f} \sum_{\substack{v=1 \\ v \neq l}}^L s^{[kv]} \sum_{j=1}^L \phi_j^{[kv]} \hat{\mathbf{g}}_j^{[kj]\dagger} \hat{\mathbf{g}}_j^{[kl]}}_{T_2} \\ & \quad + \underbrace{\sqrt{\rho_f} \sum_{j=1}^L \sum_{\substack{n=1 \\ n \neq k}}^K \hat{\mathbf{g}}_j^{[nj]\dagger} \hat{\mathbf{g}}_j^{[kl]} c_j^{[n]}}_{T_3} \\ & \quad + \underbrace{\sqrt{\rho_f} \sum_{j=1}^L \sum_{n=1}^K \hat{\mathbf{g}}_j^{[nj]\dagger} \tilde{\mathbf{g}}_j^{[kl]} c_j^{[n]}}_{T_4} + \underbrace{w^{[kl]}}_{T_5}. \end{aligned} \quad (33)$$

To make notations shorter, we denote the five terms (four sums and $w^{[kl]}$) in above expression by T_0, \dots, T_5 respectively.

First, we note that these terms are mutually uncorrelated. Indeed, since $s^{[kl]}$ is independent of any $\hat{\mathbf{g}}_i^{[ns]}$, we have

$$\begin{aligned} & \mathbb{E}[T_0^\dagger T_1] \\ &= \mathbb{E}[s^{[kl]\dagger} s^{[kl]}] \rho_f \sum_{j=1}^L \sum_{i=1}^L \phi_j^{[kl]\dagger} \phi_i^{[kl]} \mathbb{E}[\hat{\mathbf{g}}_j^{[kj]\dagger} \hat{\mathbf{g}}_i^{[kl]}]^\dagger \\ & \quad \cdot \mathbb{E}[(\hat{\mathbf{g}}_i^{[ki]\dagger} \hat{\mathbf{g}}_i^{[kl]} - \mathbb{E}[\hat{\mathbf{g}}_i^{[ki]\dagger} \hat{\mathbf{g}}_i^{[kl]}])] = 0. \end{aligned}$$

Since $s^{[kl]}$ is independent of $s^{[nv]}$ if $(k, l) \neq (n, v)$ we get

$$\begin{aligned} \mathbb{E}[T_0^\dagger T_2] &= 0, \mathbb{E}[T_0^\dagger T_3] = 0, \mathbb{E}[T_1^\dagger T_2] = 0, \\ \mathbb{E}[T_1^\dagger T_3] &= 0, \mathbb{E}[T_2^\dagger T_3] = 0. \end{aligned}$$

Since $\tilde{\mathbf{g}}_j^{[kl]}$ is uncorrelated with any $\hat{\mathbf{g}}_i^{[nv]}$, it is not difficult to check that T_4 is uncorrelated with T_0, T_1, T_2 , and T_3 . Finally, $T_5 = w^{[kl]}$ is independent from all other terms. Thus, we can rewrite (33) as

$$y^{[kl]} = s^{[kl]} \sqrt{\rho_f} \sum_{j=1}^L \phi_j^{[kl]} \mathbb{E}[\hat{\mathbf{g}}_j^{[kj]\dagger} \hat{\mathbf{g}}_j^{[kl]}] + w_{eff}^{[kl]},$$

where the effective noise has the variance

$$\text{Var}[w_{eff}^{[kl]}] = \text{Var}[T_1] + \text{Var}[T_2] + \text{Var}[T_3] + \text{Var}[T_4] + \text{Var}[T_5].$$

Using (30), we obtain

$$\begin{aligned} & \sqrt{\rho_f} \sum_{j=1}^L \phi_j^{[kl]} \mathbb{E}[\hat{\mathbf{g}}_j^{[kj]\dagger} \hat{\mathbf{g}}_j^{[kl]}] \\ &= \sqrt{\rho_f} M \rho_r \tau \sum_{j=1}^L \frac{\beta_j^{[kl]} \beta_j^{[kj]}}{1 + \sum_{s=1}^L \rho_r \tau \beta_j^{[ks]}} \phi_j^{[kl]}, \end{aligned} \quad (34)$$

which defines the quantity $\epsilon_l^{[kl]}$ in Step 3 of the LSFP protocol.

According to the protocol the l -th base station sends $\epsilon_l^{[kl]}$ to the corresponding user. So the user can use $\epsilon_l^{[kl]}$ to detect signal $s^{[kl]}$. Note that $\epsilon_l^{[kl]}$ depends only on the statistical parameters of the channel and not on instantaneous channel realizations. According to [23, Theorem 1], the worst-case uncorrelated additive noise is independent Gaussian noise with the same variance. Hence the downlink rate $R^{[kl]}$ can be lower bounded as follows

$$\begin{aligned} R^{[kl]} &= I(y^{[kl]}; s^{[kl]} | \epsilon_l^{[kl]}) \\ &\geq \log_2 \left(1 + \frac{|\epsilon_l^{[kl]}|^2}{\text{Var}[T_1] + \text{Var}[T_2] + \text{Var}[T_3] + \text{Var}[T_4] + \text{Var}[T_5]} \right). \end{aligned} \quad (35)$$

Now we proceed with finding the variances $\text{Var}[T_j], j = 1, 5$.

The term T_1 is caused by the **channel uncertainty**. The k -th user located in the l -th cell does not know the actual value of the effective channel $\hat{\mathbf{g}}_j^{[kj]\dagger} \hat{\mathbf{g}}_j^{[kl]}$, but only the expected value $\mathbb{E}[\hat{\mathbf{g}}_j^{[kj]\dagger} \hat{\mathbf{g}}_j^{[kl]}]$. So the difference, uncertainty, between the actual and expected values of the effective channel contributes to the interference. To estimate the variance of T_1 we first note that the signals $s^{[kl]}$ and $s^{[nv]}$ are independent if $(k, l) \neq$

(n, v) . Next, we note that for any $1 \leq k, n \leq K$, and $1 \leq l, v \leq L$, the vectors $\hat{\mathbf{g}}_j^{[kl]}$ and $\hat{\mathbf{g}}_i^{[nv]}$ are independent if $j \neq i$. Taking this into account we obtain

$$\begin{aligned} & \text{Var}[T_1] \\ &= \mathbb{E}[s^{[kl]} s^{[kl]\dagger}] \sum_{j=1}^L \sum_{i=1}^L \phi_j^{[kl]} \phi_i^{[kl]\dagger} \mathbb{E} \left[(\hat{\mathbf{g}}_j^{[kj]\dagger} \hat{\mathbf{g}}_j^{[kl]} - \mathbb{E}[\hat{\mathbf{g}}_j^{[kj]\dagger} \hat{\mathbf{g}}_j^{[kl]}]) \right. \\ & \quad \left. \cdot (\hat{\mathbf{g}}_i^{[ki]\dagger} \hat{\mathbf{g}}_i^{[kl]} - \mathbb{E}[\hat{\mathbf{g}}_i^{[ki]\dagger} \hat{\mathbf{g}}_i^{[kl]}])^\dagger \right] \\ &= \sum_{j=1}^L |\phi_j^{[kl]}|^2 \text{Var}[\hat{\mathbf{g}}_j^{[kj]\dagger} \hat{\mathbf{g}}_j^{[kl]}]. \end{aligned}$$

For computing $\text{Var}[\hat{\mathbf{g}}_j^{[kj]\dagger} \hat{\mathbf{g}}_j^{[kl]}]$ we note that according to (27) $\hat{\mathbf{g}}_j^{[kj]}$ is proportional to $\hat{\mathbf{g}}_j^{[kl]}$, namely

$$\hat{\mathbf{g}}_j^{[kj]} = \frac{\theta_j^{[kj]}}{\theta_j^{[kl]}} \hat{\mathbf{g}}_j^{[kl]}. \quad (36)$$

Let $\mathbf{z} = (z_1, \dots, z_M)^\top \sim \mathcal{CN}(0, \mathbf{I}_M)$. It is well know that

$$z_i \sim \mathcal{CN}(0, 1) \text{ and } z_i^\dagger z_i \sim \Gamma(3, 1),$$

and therefore $\text{Var}[z_i^\dagger z_i] = 1$. Using this, (36), and (28), we get

$$\begin{aligned} & \text{Var} \left[\hat{\mathbf{g}}_j^{[kj]\dagger} \hat{\mathbf{g}}_j^{[kl]} \right] \\ &= \frac{\rho_r \tau \beta_j^{[kl]^2}}{1 + \sum_{s=1}^L \rho_r \tau \beta_j^{[ks]}} \frac{\rho_r \tau \beta_j^{[kj]^2}}{1 + \sum_{s=1}^L \rho_r \tau \beta_j^{[ks]}} \text{Var}[\mathbf{z}^\dagger \mathbf{z}] \\ &= \frac{\rho_r \tau \beta_j^{[kl]^2}}{1 + \sum_{s=1}^L \rho_r \tau \beta_j^{[ks]}} \frac{\rho_r \tau \beta_j^{[kj]^2}}{1 + \sum_{s=1}^L \rho_r \tau \beta_j^{[ks]}} \cdot M. \quad (37) \end{aligned}$$

Thus

$$\begin{aligned} & \text{Var}[T_1] \\ &= M \sum_{j=1}^L |\phi_j^{[kl]}|^2 \frac{\rho_r \tau \beta_j^{[kl]^2}}{1 + \sum_{s=1}^L \rho_r \tau \beta_j^{[ks]}} \frac{\rho_r \tau \beta_j^{[kj]^2}}{1 + \sum_{s=1}^L \rho_r \tau \beta_j^{[ks]}}. \quad (38) \end{aligned}$$

Next, we consider the term T_2 . This term is caused by the **pilot contamination effect**. Since the k -th users in cells j and l use the same training sequence the vector $\hat{\mathbf{g}}_j^{[kj]}$ is correlated with the vector $\hat{\mathbf{g}}_j^{[kl]}$ even if $l \neq j$. Taking into account the same facts about signals $s^{[nv]}$ and vectors $\hat{\mathbf{g}}_i^{[nv]}$ that we used in the derivation of $\text{Var}[T_1]$, we obtain

$$\begin{aligned} & \text{Var}[T_2] \\ &= \sum_{\substack{l=1 \\ v \neq l}}^L \mathbb{E}[s^{[kv]} s^{[kv]\dagger}] \sum_{j=1}^L \sum_{i=1}^L \phi_j^{[kv]} \phi_i^{[kv]\dagger} \mathbb{E}[\hat{\mathbf{g}}_j^{[kj]\dagger} \hat{\mathbf{g}}_j^{[kl]} \hat{\mathbf{g}}_i^{[kl]\dagger} \hat{\mathbf{g}}_i^{[ki]}] \\ &= \sum_{\substack{l=1 \\ v \neq l}}^L \sum_{j=1}^L \sum_{\substack{i=1 \\ i \neq j}}^L \phi_j^{[kv]} \phi_i^{[kv]\dagger} \mathbb{E}[\hat{\mathbf{g}}_j^{[kj]\dagger} \hat{\mathbf{g}}_j^{[kl]}] \mathbb{E}[\hat{\mathbf{g}}_i^{[kl]\dagger} \hat{\mathbf{g}}_i^{[ki]}] \\ & \quad + \sum_{\substack{l=1 \\ v \neq l}}^L \sum_{j=1}^L |\phi_j^{[kv]}|^2 \mathbb{E}[\hat{\mathbf{g}}_j^{[kj]\dagger} \hat{\mathbf{g}}_j^{[kl]} \hat{\mathbf{g}}_j^{[kl]\dagger} \hat{\mathbf{g}}_j^{[kj]}]. \end{aligned}$$

Using (37) and (30), we obtain

$$\begin{aligned} & \mathbb{E}[\hat{\mathbf{g}}_j^{[kj]\dagger} \hat{\mathbf{g}}_j^{[kl]} \hat{\mathbf{g}}_j^{[kl]\dagger} \hat{\mathbf{g}}_j^{[kj]}] \\ &= \text{Var}[\hat{\mathbf{g}}_j^{[kj]\dagger} \hat{\mathbf{g}}_j^{[kl]}] + |\mathbb{E}[\hat{\mathbf{g}}_j^{[kj]\dagger} \hat{\mathbf{g}}_j^{[kl]}]|^2 \\ &= M \cdot \frac{\rho_r \tau \beta_j^{[kl]^2}}{1 + \sum_{s=1}^L \rho_r \tau \beta_j^{[ks]}} \cdot \frac{\rho_r \tau \beta_j^{[kj]^2}}{1 + \sum_{s=1}^L \rho_r \tau \beta_j^{[ks]}} \\ & \quad + \left(\frac{M \rho_r \tau \beta_j^{[kl]} \beta_j^{[kj]}}{1 + \sum_{s=1}^L \rho_r \tau \beta_j^{[ks]}} \right)^2. \end{aligned}$$

From this, we have

$$\begin{aligned} & \text{Var}[T_2] \\ &= \sum_{\substack{l=1 \\ v \neq l}}^L \left| \sum_{j=1}^L \frac{M \rho_r \tau \beta_j^{[kj]} \beta_j^{[kl]}}{1 + \sum_{s=1}^L \rho_r \tau \beta_j^{[ks]}} \phi_j^{[kv]} \right|^2 \\ & \quad + \sum_{\substack{l=1 \\ v \neq l}}^L M \sum_{j=1}^L \frac{\rho_r \tau \beta_j^{[kl]^2}}{1 + \sum_{s=1}^L \rho_r \tau \beta_j^{[ks]}} \frac{\rho_r \tau \beta_j^{[kj]^2}}{1 + \sum_{s=1}^L \rho_r \tau \beta_j^{[ks]}} |\phi_j^{[kv]}|^2. \quad (39) \end{aligned}$$

Let us consider now the term T_3 , which is caused by the **nonorthogonality of channel vectors**. In the asymptotic regime, as M tends to infinity, the normalized inner-product of vectors $\hat{\mathbf{g}}_j^{[kl]}$ and $\hat{\mathbf{g}}_j^{[nj]}$ almost surely converges to zero. For finite M , however, this is not the case and T_3 may significantly contribute to the interference. From (32), we have

$$\mathbb{E}[|c_j^{[n]}|^2] = \sum_{v=1}^L \sum_{u=1}^L \phi_j^{[nv]} \phi_j^{[nu]\dagger} \mathbb{E}[s^{[nv]} s^{[nu]\dagger}] = \sum_{v=1}^L |\phi_j^{[nv]}|^2.$$

Using this, (30), and the fact that $\hat{\mathbf{g}}_j^{[nj]}$ and $\hat{\mathbf{g}}_j^{[kl]}$ are uncorrelated, we obtain

$$\begin{aligned} & \text{Var}[T_3] \\ &= \sum_{j=1}^L \sum_{\substack{n=1 \\ n \neq k}}^K \mathbb{E}[\hat{\mathbf{g}}_j^{[nj]\dagger} \hat{\mathbf{g}}_j^{[kl]} \hat{\mathbf{g}}_j^{[kl]\dagger} \hat{\mathbf{g}}_j^{[nj]}] \cdot \mathbb{E}[|c_j^{[n]}|^2] \\ &= \sum_{j=1}^L \sum_{\substack{n=1 \\ n \neq k}}^K \mathbb{E}[\text{Tr}(\hat{\mathbf{g}}_j^{[nj]} \hat{\mathbf{g}}_j^{[nj]\dagger} \hat{\mathbf{g}}_j^{[kl]} \hat{\mathbf{g}}_j^{[kl]\dagger})] \cdot \mathbb{E}[|c_j^{[n]}|^2] \\ &= \sum_{j=1}^L \sum_{\substack{n=1 \\ n \neq k}}^K \text{Tr} \left(\mathbb{E}[\hat{\mathbf{g}}_j^{[nj]} \hat{\mathbf{g}}_j^{[nj]\dagger}] \mathbb{E}[\hat{\mathbf{g}}_j^{[kl]} \hat{\mathbf{g}}_j^{[kl]\dagger}] \right) \cdot \mathbb{E}[|c_j^{[n]}|^2] \\ &= M \sum_{j=1}^L \sum_{\substack{n=1 \\ n \neq k}}^K \frac{\rho_r \tau \beta_j^{[kl]^2}}{1 + \sum_{s=1}^L \rho_r \tau \beta_j^{[ks]}} \cdot \frac{\rho_r \tau \beta_j^{[nj]^2}}{1 + \sum_{s=1}^L \rho_r \tau \beta_j^{[ks]}} \\ & \quad \cdot \sum_{v=1}^L |\phi_j^{[kv]}|^2. \end{aligned}$$

Term T_4 is caused by **estimation errors of channel vectors**. Since $\hat{\mathbf{g}}_j^{[kl]}$ is uncorrelated with any $\hat{\mathbf{g}}_i^{[nv]}$, using (27) and (29)

we obtain

$$\begin{aligned} \text{Var}[T_4] &= \sum_{j=1}^L \sum_{n=1}^K \text{Tr} \left(\mathbb{E}[\hat{\mathbf{g}}_j^{[nj]} \hat{\mathbf{g}}_j^{[nj]\dagger}] \mathbb{E}[\hat{\mathbf{g}}_j^{[kl]} \hat{\mathbf{g}}_j^{[kl]\dagger}] \right) \cdot \mathbb{E}[|c_j^{[n]}|^2] \\ &= M \sum_{j=1}^L \sum_{n=1}^K \left(\beta_j^{[kl]} - \frac{\rho_r \tau \beta_j^{[kl]^2}}{1 + \sum_{s=1}^L \rho_r \tau \beta_j^{[ks]}} \right) \\ &\quad \cdot \frac{\rho_r \tau \beta_j^{[nj]^2}}{1 + \sum_{s=1}^L \rho_r \tau \beta_j^{[ks]}} \cdot \sum_{v=1}^L |\phi_j^{[kv]}|^2. \end{aligned}$$

Finally, the **power of additive noise** $w^{[kl]}$ is $\text{Var}[T_5] = \text{Var}[w^{[kl]}] = 1$.

Now, after some computations, we obtain from (35) the following theorem.

Theorem 7: If the conjugate beamforming precoding is used in Step 6 of LSFP then the downlink transmission rate $R^{[kl]}$ is lower bounded by

$$R_D^{[kl]} \geq \log_2(1 + \text{SINR}_D^{[kl]}), \quad k = 1, K, \quad l = 1, L,$$

where

$$\text{SINR}_D^{[kl]} = \frac{\rho_f M^2 \rho_r^2 \tau^2 \left| \sum_{j=1}^L \frac{\beta_j^{[kl]} \beta_j^{[kj]}}{1 + \sum_{s=1}^L \rho_r \tau \beta_j^{[ks]}} \phi_j^{[kl]} \right|^2}{M^2 I_1 + M I_2 + 1}, \quad (40)$$

and

$$I_1 = \rho_f \rho_r^2 \tau^2 \sum_{\substack{v=1 \\ v \neq l}}^L \left| \sum_{j=1}^L \frac{\beta_j^{[kl]} \beta_j^{[kj]}}{1 + \sum_{s=1}^L \rho_r \tau \beta_j^{[ks]}} \phi_j^{[kv]} \right|^2$$

and

$$I_2 = \rho_f \rho_r \tau \sum_{j=1}^L \sum_{n=1}^K \frac{\beta_j^{[nj]^2}}{1 + \sum_{s=1}^L \rho_r \tau \beta_j^{[ns]}} \beta_j^{[kl]} \sum_{v=1}^L |\phi_j^{[nv]}|^2.$$

It is instructive to apply Theorem 7 for the cases when LSFP is not used and when ZF-LSFP is used.

B. No LSFP and ZF-LSFP

If we do not use LSFP then the matrices $\Phi^{[k]}$ are diagonal. Hence, taking into account (30) and the power constraint

$$\mathbb{E}[|\hat{\mathbf{g}}_j^{[kj]} c_j^{[k]}|^2] = \mathbb{E}[|\hat{\mathbf{g}}_j^{[kj]} \phi_j^{[kj]} s^{[kj]}|^2] = 1,$$

we conclude that

$$\phi_j^{[kl]} = \delta_{jl} \frac{(1 + \sum_{s=1}^L \rho_r \tau \beta_j^{[ns]})^{1/2}}{\sqrt{M \rho_r \tau \beta_j^{[kj]}}}, \quad (41)$$

where δ_{jl} is Kronecker's delta. The numerator of (40) will have the form

$$\rho_f M \rho_r \tau \frac{\beta_l^{[kl]^2}}{1 + \sum_{s=1}^L \rho_r \tau \beta_l^{[ks]}}$$

and

$$\begin{aligned} I_1 &= \frac{\rho_f \rho_r \tau}{M} \sum_{\substack{v=1 \\ v \neq l}}^L \frac{\beta_v^{[kl]^2}}{1 + \sum_{s=1}^L \rho_r \tau \beta_v^{[ks]}}, \\ I_2 &= \frac{\rho_f}{M} \sum_{j=1}^L \sum_{n=1}^K \frac{\beta_j^{[nj]^2}}{1 + \sum_{s=1}^L \rho_r \tau \beta_j^{[ns]}} \beta_j^{[kl]} \\ &\quad \sum_{v=1}^L \frac{1 + \sum_{s=1}^L \rho_r \tau \beta_j^{[ns]}}{\rho_r \tau \beta_j^{[nj]}}. \end{aligned}$$

Let now $M \rightarrow \infty$. In this case we get

$$\lim_{M \rightarrow \infty} \text{SINR}_{D,NO}^{[kl]} = \frac{\beta_l^{[kl]} / (1 + \sum_{s=1}^L \rho_r \tau \beta_l^{[ks]})}{\sum_{v \neq l}^L \beta_v^{[kl]^2} / (1 + \sum_{s=1}^L \rho_r \tau \beta_v^{[ks]})}.$$

Thus we again obtained (9) and again we see that for very large number of base station antennas the interference is completely defined by the pilot contamination effect.

Let us consider ZF-LSFP. Let

$$\mu_j^{[k]} = \frac{\beta_j^{[kj]}}{1 + \sum_{s=1}^L \rho_r \tau \beta_j^{[ks]}}$$

and define $L \times L$ matrix

$$\mathbf{B}^{[k]} = \begin{pmatrix} \beta_1^{[k1]} \mu_1^{[k]} & \dots & \beta_L^{[k1]} \mu_L^{[k]} \\ \vdots & & \vdots \\ \beta_1^{[kL]} \mu_1^{[k]} & \dots & \beta_L^{[kL]} \mu_L^{[k]} \end{pmatrix}. \quad (42)$$

Let further

$$\Phi^{[k]} = \sqrt{\rho_A} \mathbf{B}^{[k]-1}, \quad k = 1, K,$$

where ρ_A is a normalization factor to insure the constraint (12). With such $\Phi^{[k]}$ the numerator of (40) and I_1 are

$$\rho_f M^2 \rho_r^2 \rho_A \tau^2 \quad \text{and} \quad I_1 = 0.$$

In the asymptotic regime, as $M \rightarrow \infty$ we get

$$\lim_{M \rightarrow \infty} \text{SINR}_{D,ZF-LSFP}^{[kl]} = \lim_{M \rightarrow \infty} \frac{\rho_f M^2 \rho_r^2 \tau^2}{M I_2} = \infty.$$

So, similar to Theorem 4, we obtained that in the asymptotic regime ZF-LSFP allows achieving infinite SINRs for all users.

Remark 3: The matrix (42) has a slightly different form compared with (14) because we assumed that the user knows only the expected gain of the effective channel, that is the quantity $\epsilon_i^{[kl]}$. In contrast, in Section III it is implicitly assumed that the user knows the actual value of the effective channels $\hat{\mathbf{g}}_j^{[kl]} \hat{\mathbf{g}}_j^{[kl]}$.

C. Optimization Problem

We can slightly simplify notation if we replace $\phi_j^{[kl]}$ with

$$\alpha_j^{[kl]} = \frac{\sqrt{\rho_r \tau} \beta_j^{[kj]}}{1 + \sum_{s=1}^L \rho_r \tau \beta_j^{[ks]}} \phi_j^{[kl]}.$$

This replacement does not cause any problems since all the quantities used in the above expression are assumed being known at the j -th base station. After this replacement we get

$$\text{SINR}_D^{[kl]} = \frac{M \rho_f \rho_r \tau \left| \sum_{j=1}^L \beta_j^{[kl]} \alpha_j^{[kl]} \right|^2}{M J_1 + J_2 + 1/M}, \quad (43)$$

where

$$J_1 = \rho_f \rho_r \tau \sum_{\substack{v=1 \\ v \neq l}}^L \left| \sum_{j=1}^L \beta_j^{[kl]} \alpha_j^{[kv]} \right|^2,$$

and

$$J_2 = \rho_f \sum_{j=1}^L \sum_{n=1}^K \beta_j^{[kl]} \left(1 + \sum_{s=1}^L \rho_r \tau \beta_j^{[ks]} \right) \left(\sum_{v=1}^L |\phi_j^{[nv]}|^2 \right).$$

With this notations the average power of the j -th base station is the following function of the large-scale fading coefficients and the LSFP coefficients:

$$\begin{aligned} \gamma_j &= \sum_{k=1}^K \mathbb{E}[|\mathbf{g}_j^{[kj]} c_j^{[k]}|^2] \\ &= M \sum_{k=1}^K \left(1 + \sum_{s=1}^L \rho_r \tau \beta_j^{[ks]} \right) \left(\sum_{v=1}^L |\alpha_j^{[kv]}|^2 \right). \end{aligned} \quad (44)$$

Using (44) one may formulate different optimization problems with base station power constraints. In particular, in Part II of this paper [2] we consider the following problem

$$\max_{\alpha_j^{[nr]}, n=1, K, j, r=1, L} \min_{k=1, K, l=1, L} \text{SINR}_D^{[kl]}$$

subject to the constraints

$$\gamma_j \leq 1, j = 1, L.$$

D. First Simulation Results

Since ZF-LSFP allows achieving infinite SINRs when $M \rightarrow \infty$ it is natural to ask what it gives us when M is finite. In order to answer this question we generate random large-scale fading coefficients and use Theorem 40 for finding corresponding downlink rates $R_D^{[kl]}$ when LSFP is not used (No LSFP) and when ZF-LSFP is used. In Fig. 4 and Fig. 5, we present simulation results for the CDFs of $R_D^{[kl]}$, $k = 1, K, l = 1, L$, and the CDF of the minimum rate $\min_{k,l} R_D^{[kl]}$, respectively. We plot achievable rates and CDF in horizontal and vertical axis, respectively. In these simulations, we assumed $K = 10$.

It can be observed from both figures that by increasing the number of antennas we significantly improve the performance of ZF-LSFP. In Fig. 4, ZF-LSFP achieves 5%-outage rate around 10^{-6} bits per channel use at $M = 100$; the achievable rate is improved to around 10^{-2} bits per channel use with $M = 10^6$ antennas. On the other hand, the achievable rate of no-LSFP is saturated when M is getting very large.

According to Fig. 4, when we consider the rates of all users, the 5%-outage rate of no-LSFP is larger than the 5%-outage rate of ZF-LSFP at $M = 100, 10^4$ and only at $M = 10^5$ ZF-LSFP starts outperforming No LSFP. In the case of CDFs of minimum rates $\min_{k,l} R_D^{[kl]}$ shown in Fig. 5, ZF-LSFP has better performance than No LSFP already at $M = 10^4$, which is still a very large number of antennas.

Thus we conclude that in a regime with a practical number of antennas, e.g. $M = 100$ and smaller, the ZF-LSFP performs worse than No LSFP approach. It is a natural question to ask whether an LSFP different from ZF-LSFP can give any

gain in such scenario, or LSFP is only a theoretical tool for investigation of the asymptotic case $M \rightarrow \infty$. We answer to this question in Part II of the paper [2]. We will show that properly designed LSFP gives very significant gain over other methods of interference reduction.

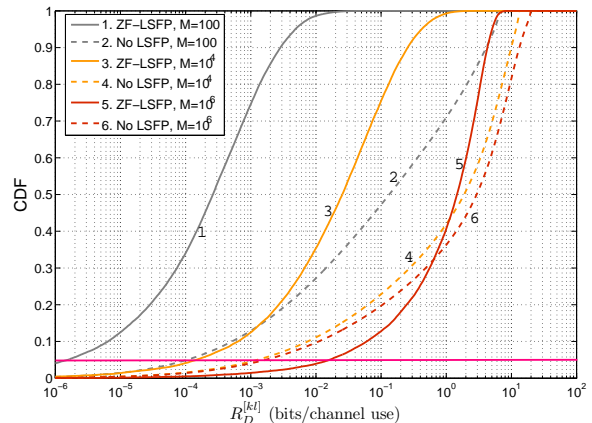


Fig. 4. The CDF of the achievable rate $R_D^{[kl]} = \log(1 + \text{SINR}^{[kl]})$ for two existing methods with different number of antennas.

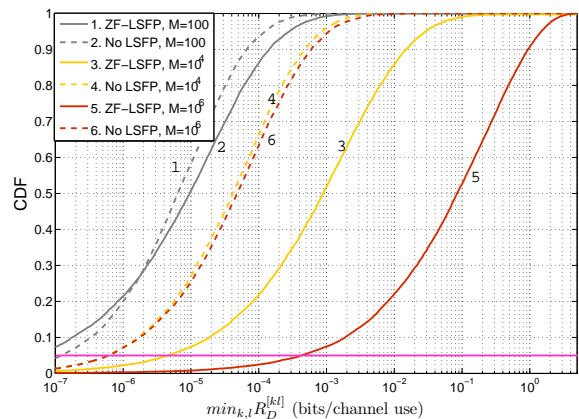


Fig. 5. The CDF of the achievable rate $R_D^{[kl]} = \log(1 + \text{SINR}^{[kl]})$ for two existing methods with different number of antennas.

E. Performance of Large-Scale Fading Decoding with finite M

Denote the (l, v) -th entry of matrix $\Omega^{[k]}$ by $\omega_l^{[kv]}$. Similar to the downlink case we obtain the following theorem.

Theorem 8:

$$R_U^{[kl]} \geq \log_2(1 + \text{SINR}_{UL}^{[kl]}), \quad k = 1, K, l = 1, L,$$

where

$$\text{SINR}_U^{[kl]} = \frac{M^2 \rho_r^3 \tau^2 \left| \sum_{v=1}^L \frac{\beta_v^{[kv]} \beta_v^{[kl]}}{1 + \sum_{s=1}^L \rho_r \tau \beta_v^{[ks]}} \omega_l^{[kv]} \right|^2}{M^2 I_1 + M I_2}, \quad (45)$$

and

$$I_1 = \rho_r^3 \tau^2 \sum_{\substack{j=1 \\ j \neq l}}^L \left| \sum_{v=1}^L \frac{\beta_v^{[kv]} \beta_v^{[kj]}}{1 + \sum_{s=1}^L \rho_r \tau \beta_v^{[ks]}} \omega_l^{[kv]} \right|^2,$$

$$I_2 = \sum_{v=1}^L |\omega_l^{[kv]}|^2 \frac{\rho_r \tau \beta_v^{[kv]^2}}{1 + \sum_{s=1}^L \rho_r \tau \beta_v^{[ks]}} \left(1 + \rho_r \sum_{j=1}^L \sum_{n=1}^K \beta_v^{[nj]} \right).$$

Before presenting a formal proof of this theorem we would like to note that the important distinction of this result from Theorem 40. The coefficients $\omega_l^{[kv]}$ appear only in $\text{SINR}_U^{[kl]}$ and not in any other $\text{SINR}_U^{[nj]}$. Thus optimal LSFP coefficients $\omega_l^{[kv]}$, $v = 1, L$, can be chosen independently for each user, which significantly simplify search of optimal coefficients.

We also would like to note that we can slightly simplify expression for $\text{SINR}_U^{[kl]}$ if replace $\omega_l^{[kv]}$ with

$$\omega_l^{[kv]*} = \frac{\sqrt{\rho_r \tau M} \beta_v^{[kv]}}{1 + \sum_{s=1}^L \rho_r \tau \beta_v^{[ks]}} \omega_l^{[kv]}.$$

In this case we get

$$\text{SINR}_U^{[kl]} = \frac{M \rho_r^2 \tau \left| \sum_{v=1}^L \beta_v^{[kl]} \omega_l^{[kv]*} \right|^2}{M J_1 + J_2}, \quad (46)$$

where

$$J_1 = \rho_r^2 \tau \sum_{\substack{j=1 \\ j \neq l}}^L \left| \sum_{v=1}^L \beta_v^{[kj]} \omega_l^{[kv]*} \right|^2$$

and

$$J_2 = \sum_{v=1}^L |\omega_l^{[kv]*}|^2 \left(1 + \sum_{s=1}^L \rho_r \tau \beta_v^{[ks]} \right) \left(1 + \rho_r \sum_{j=1}^L \sum_{n=1}^K \beta_v^{[nj]} \right).$$

Finally, it is instructive to consider the expression (46) for the cases of NO LSFP and ZF-LSFP. If we do not use LSFP then $\omega_l^{[kv]} = \delta_{lv}$. Substituting such $\omega_l^{[kv]} = \delta_{lv}$ into (46), in the regime $M \rightarrow \infty$ we get for the expression (11) from Section III-A. In the case of ZF-LSFP we chose $\omega_l^{[kv]}$ according to (25). Using these coefficients in (46) we get the result of Theorem 6 from Section III.

The proof is similar to the proof of Theorem 7. However, as we noted above, the LSFP coefficients $\omega_l^{[kv]}$ appear in $\text{SINR}_U^{[kl]}$ in a different way than in Theorem 40. So it is important to carefully track all indices involved into the computations. The proof is in Appendix B.

V. APPENDIX A

Let $\mathcal{R} = \{r_1, \dots, r_N\}$ be a constellation of signals such that $\min_{i,j} \text{dist}(r_i, r_j) \geq \Delta$ for some positive real Δ and N is an arbitrary integer.

Before presenting a proof of Lemma 5, we would like to note that when we deal with mutual information or entropy functions we not always can replace a random variable, say x_M , with its limit value. For example, let x_M be defined by

$$\begin{aligned} \Pr(x_M = -1 - 1/M) &= \Pr(x_M = -1 + 1/M) \\ &= \Pr(x_M = 1 - 1/M) = \Pr(x_M = 1 + 1/M) = 1/4. \end{aligned}$$

It is easy to see that

$$\lim_{M \rightarrow \infty} x_M \stackrel{\text{a.s.}}{=} x,$$

where x is a random variable defined by

$$\Pr(x = -1) = \Pr(x = 1) = \frac{1}{2}.$$

At the same time, in the case of the binary entropy, we have

$$H_2(x) = - \sum_{x \in \{-1, 1\}} \Pr(x) \log_2 \Pr(x) = 1,$$

while $H_2(x_M) = 2$ for any M and therefore

$$\lim_{M \rightarrow \infty} H_2(x_M) = 2.$$

Thus we have

$$H_2(\lim_{M \rightarrow \infty} x_M) \neq \lim_{M \rightarrow \infty} H_2(x_M).$$

This example shows that the statement of Lemma 5 is not trivial and indeed needs a proof.

Let us define for some positive ϕ and β the events A_M , W_M by $a_M \in [1 - \phi, 1 + \phi]$ and $w_M \in [-\beta, \beta]$ respectively. We would like to remind that

$$\lim_{M \rightarrow \infty} a_M \stackrel{\text{a.s.}}{=} 1 \text{ and } \lim_{M \rightarrow \infty} w_M \stackrel{\text{a.s.}}{=} 0$$

imply that

$$\lim_{M \rightarrow \infty} \Pr(A_M^c) = 0, \text{ and} \quad (47)$$

$$\lim_{M \rightarrow \infty} \Pr(W_M^c) = 0. \quad (48)$$

We also have

$$\lim_{M \rightarrow \infty} \Pr(A_M \cap W_M) = 1. \quad (49)$$

Indeed

$$\begin{aligned} \Pr(A_M \cap W_M) &= \Pr((A_M^c \cup W_M^c)^c) \\ &= 1 - \Pr(A_M^c \cup W_M^c) \geq 1 - \Pr(A_M^c) - \Pr(W_M^c) = 1. \end{aligned}$$

In a similar way one can show that

$$\lim_{M \rightarrow \infty} \Pr(A_M \cap W_M^c) = 0. \quad (50)$$

Proof: (Lemma 5) Below we show that for any given Δ , by choosing sufficiently large M , we can make $I(s_M; s)$ being arbitrary close to $H(s)$.

To make notation short we assume that N is even and the signals \mathcal{R} are evenly spaced on the real line that is

$$\mathcal{R} = \{-N/2 \cdot \Delta, -(N/2 - 1)\Delta, \dots, (N/2 - 1)\Delta, N/2 \cdot \Delta\}.$$

Generalizations for unevenly spaced signals and for complex signals are straightforward.

For a given s_M , let $q_M \in \mathcal{R}$ be such that

$$\text{dist}(q_M, s_M) \leq \text{dist}(s', s_M) \text{ for any } s' \in \mathcal{R} \setminus q_M.$$

In other words q_M is obtained by demodulation of s_M with respect to \mathcal{R} . According to the data processing inequality we have

$$I(q_M, s) \leq I(s_M, s) \leq H(s). \quad (51)$$

Next,

$$I(q_M, s) = H(s) - H(s|q_M),$$

Denote by $P_Q(\cdot)$ the PMF of q_M . Then

$$\begin{aligned} & H(s|q_M) \\ &= \sum_{q_M \in \mathcal{R}} P_Q(q_M) \sum_{s \in \mathcal{R}} P_{S|Q}(s|q_M) \log P_{S|Q}(s|q_M) \\ &= \sum_{q_M \in \mathcal{R}} P_Q(q_M) [P_{S|Q}(s = q_M|q_M) \log P_{S|Q}(s = q_M|q_M) \\ &\quad + \sum_{s' \in \mathcal{R} \setminus q_M} P_{S|Q}(s'|q_M) \log P_{S|Q}(s'|q_M)] \end{aligned}$$

The conditional probability $P_{S|Q}(s = q_M|q_M)$ can be written as

$$\begin{aligned} & P_{S|Q}(s = q_M|q_M) \\ &= \frac{P_S(q_M)P_{Q|S}(q_M|s = q_M)}{P_S(q_M)P_{Q|S}(q_M|s = q_M) + \sum_{s' \in \mathcal{R} \setminus q_M} P_S(s')P_{Q|S}(q_M|s')} \end{aligned}$$

First, we estimate $P_S(q_M)P_{Q|S}(q_M|s')$, $s' \neq q_M$. From the definition of q_M it follows that

$$P_{Q|S}(q_M|s') = \Pr(a_M s' + w_M \in (q_M - \Delta/2, q_M + \Delta/2)).$$

Let us assume that $q_M = (n-1)\Delta$ and $s' = n\Delta$ for some positive integer n . If $a_M \geq 1 - 1/4n$. Then in order to have

$$\begin{aligned} a_M s' + w_M &\in [q_M - \Delta/2, q_M + \Delta/2] \\ &= [(n-1)\Delta - \Delta/2, (n-1)\Delta + \Delta/2], \end{aligned}$$

we need that $w_M < -\Delta/4$. Similarly, if $a_M \leq 1 + 1/4n$ we have to have $w_M > -7\Delta/4$. Hence, if $a_M \in [1 - 1/4n, 1 + 1/4n]$ then w_M can not be outside of the interval $(-7\Delta/4, -\Delta/4)$. Thus

$$\begin{aligned} & P_{Q|S}(q_M = (n-1)\Delta|s' = n\Delta) \\ &\leq \Pr(a_M \in [1 - 1/4n, 1 + 1/4n] \text{ and } w_M \in (-7/4\Delta, -1/4\Delta)) \\ &\quad + \Pr(a_M \notin [1 - 1/4n, 1 + 1/4n]). \end{aligned}$$

Applying now (50) and (47) to the above terms, we get

$$\lim_{M \rightarrow \infty} P_{Q|S}(q_M = (n-1)\Delta|s' = n\Delta) = 0.$$

For any other $s' \in \mathcal{R} \setminus q_M$ we can use similar arguments that lead to

$$\lim_{M \rightarrow \infty} P_{Q|S}(q_M|s') = 0.$$

Hence, taking into account that the number of terms in the sum is countable, we get

$$\lim_{M \rightarrow \infty} \sum_{s' \in \mathcal{R} \setminus q_M} P_S(s')P_{Q|S}(q_M|s') = 0. \quad (52)$$

Using the same type of arguments we can show that

$$\begin{aligned} & P_{Q|S}(q_M|s = q_M) \\ &= \Pr(a_M q_M + w_M \in (q_M - \Delta/2, q_M + \Delta/2)) \\ &\geq \Pr(a_M \in [1 - 1/4n, 1 + 1/4n] \text{ and } w_M \in [-\Delta/4, \Delta/4]). \end{aligned}$$

Applying (49) to this lower bound we conclude that it converges to 1. Thus

$$\lim_{M \rightarrow \infty} P_{Q|S}(q_M|s = q_M) = 1. \quad (53)$$

From (53) and (52) we get

$$\lim_{M \rightarrow \infty} P_{S|Q}(s = q_M|q_M) = 1.$$

and further

$$\lim_{M \rightarrow \infty} P_{S|Q}(s = q_M|q_M) \log P_{S|Q}(s = q_M|q_M) = 0. \quad (54)$$

For $s' \neq q_M$ we have

$$\begin{aligned} & P_{S|Q}(s'|q_M) \\ &= \frac{P_S(s')P_{Q|S}(q_M|s')}{P_S(q_M)P_{Q|S}(q_M|s = q_M) + \sum_{s'' \in \mathcal{R} \setminus q_M} P_S(s'')P_{Q|S}(q_M|s'')}. \end{aligned}$$

Using (52) and (53) we obtain

$$\lim_{M \rightarrow \infty} P_{S|Q}(s'|q_M) = 0,$$

and further

$$\lim_{M \rightarrow \infty} P_{S|Q}(s'|q_M) \log P_{S|Q}(s'|q_M) = 0. \quad (55)$$

From (54) and (55) it follows that

$$\lim_{M \rightarrow \infty} H(s|q_M) = 0 \text{ and } \lim_{M \rightarrow \infty} I(q_M; s) = H(s),$$

which, together with (51), finishes the proof. \blacksquare

VI. APPENDIX B

Proof: of Theorem 8. The l -th base station receives the signal

$$\mathbf{y}_l = \sqrt{\rho_r} \sum_{j=1}^L \sum_{n=1}^K \mathbf{g}_l^{[nj]} x^{[nj]} + \mathbf{w}_l.$$

After applying the matched filter $\hat{\mathbf{g}}_l^{[kl]}$ it gets

$$\tilde{x}^{[kl]} = \hat{\mathbf{g}}_l^{[kl]\dagger} \mathbf{y}_l = \sqrt{\rho_r} \sum_{j=1}^L \sum_{n=1}^K \hat{\mathbf{g}}_l^{[kl]\dagger} \mathbf{g}_l^{[nj]} x^{[nj]} + \hat{\mathbf{g}}_l^{[kl]\dagger} \mathbf{w}_l,$$

where $\mathbf{w}_l \sim \mathcal{CN}(0, \mathbf{I}_M)$. The network controller collects these estimates and applies pilot contamination decoding:

$$\begin{aligned}
\hat{x}^{[kl]} &= \sum_{v=1}^L \omega_l^{[kv]} \hat{x}^{[kv]} \\
&= \sqrt{\rho_r} \sum_{v=1}^L \sum_{j=1}^L \sum_{n=1}^K \omega_l^{[kv]} \hat{\mathbf{g}}_v^{[kv]\dagger} \mathbf{g}_v^{[nj]} x^{[nj]} + \sum_{v=1}^L \omega_l^{[kv]} \hat{\mathbf{g}}_v^{[kv]\dagger} \mathbf{w}_v \\
&= \sqrt{\rho_r} \sum_{v=1}^L \sum_{j=1}^L \sum_{n=1}^K \omega_l^{[kv]} \hat{\mathbf{g}}_v^{[kv]\dagger} \hat{\mathbf{g}}_v^{[nj]} x^{[nj]} \\
&\quad + \sqrt{\rho_r} \sum_{v=1}^L \sum_{j=1}^L \sum_{n=1}^K \omega_l^{[kv]} \hat{\mathbf{g}}_v^{[kv]\dagger} \tilde{\mathbf{g}}_v^{[nj]} x^{[nj]} + \sum_{v=1}^L \omega_l^{[kv]} \hat{\mathbf{g}}_v^{[kv]\dagger} \mathbf{w}_v \\
&= s^{[kl]} \sqrt{\rho_r} \sum_{v=1}^L \omega_l^{[kv]} \hat{\mathbf{g}}_v^{[kv]\dagger} \hat{\mathbf{g}}_v^{[kl]} \\
&\quad + \sqrt{\rho_r} \sum_{v=1}^L \sum_{\substack{j=1 \\ j \neq l}}^L \sum_{n=1}^K \omega_l^{[kv]} \hat{\mathbf{g}}_v^{[kv]} \hat{\mathbf{g}}_v^{[nj]} s^{[nj]} \\
&\quad + \sqrt{\rho_r} \sum_{v=1}^L \sum_{j=1}^L \sum_{\substack{n=1 \\ n \neq k}}^K \omega_l^{[kv]} \hat{\mathbf{g}}_v^{[kv]} \hat{\mathbf{g}}_v^{[nj]} s^{[nj]} \\
&\quad + \sqrt{\rho_r} \sum_{v=1}^L \sum_{j=1}^L \sum_{n=1}^K \omega_l^{[kv]} \hat{\mathbf{g}}_v^{[kv]\dagger} \tilde{\mathbf{g}}_v^{[nj]} x^{[nj]} + \sum_{v=1}^L \omega_l^{[kv]} \hat{\mathbf{g}}_v^{[kv]\dagger} \mathbf{w}_v \\
&= s^{[kl]} \sqrt{\rho_r} \sum_{v=1}^L \omega_l^{[kv]} \mathbb{E}[\hat{\mathbf{g}}_v^{[kv]\dagger} \hat{\mathbf{g}}_v^{[kl]}] \\
&\quad + s^{[kl]} \sqrt{\rho_r} \sum_{v=1}^L \omega_l^{[kv]} (\hat{\mathbf{g}}_v^{[kv]\dagger} \hat{\mathbf{g}}_v^{[kl]} - \mathbb{E}[\hat{\mathbf{g}}_v^{[kv]\dagger} \hat{\mathbf{g}}_v^{[kl]}]) \\
&\quad + \sqrt{\rho_r} \sum_{v=1}^L \sum_{\substack{j=1 \\ j \neq l}}^L \sum_{n=1}^K \omega_l^{[kv]} \hat{\mathbf{g}}_v^{[kv]} \hat{\mathbf{g}}_v^{[nj]} s^{[nj]} \\
&\quad + \sqrt{\rho_r} \sum_{v=1}^L \sum_{j=1}^L \sum_{\substack{n=1 \\ n \neq k}}^K \omega_l^{[kv]} \hat{\mathbf{g}}_v^{[kv]} \hat{\mathbf{g}}_v^{[nj]} s^{[nj]} \\
&\quad + \sqrt{\rho_r} \sum_{v=1}^L \sum_{j=1}^L \sum_{n=1}^K \omega_l^{[kv]} \hat{\mathbf{g}}_v^{[kv]\dagger} \tilde{\mathbf{g}}_v^{[nj]} x^{[nj]} + \sum_{v=1}^L \omega_l^{[kv]} \hat{\mathbf{g}}_v^{[kv]\dagger} \mathbf{w}_v. \tag{56}
\end{aligned}$$

Denote the terms of this expression by Q_0, \dots, Q_5 . Similar to the downlink case it is not difficult to prove that these terms are mutually uncorrelated. Hence we can rewrite (56) in the form:

$$\hat{x}^{[kl]} = s^{[kl]} \sqrt{\rho_r} \sum_{v=1}^L \omega_l^{[kv]} \mathbb{E}[\hat{\mathbf{g}}_v^{[kv]\dagger} \hat{\mathbf{g}}_v^{[kl]}] + w_{eff}^{[kl]}$$

and

$$\begin{aligned}
&\text{Var}[w_{eff}^{[kl]}] \\
&= \text{Var}[Q_1] + \text{Var}[Q_2] + \text{Var}[Q_3] + \text{Var}[Q_4] + \text{Var}[Q_5].
\end{aligned}$$

Again using [23, Theorem 1] we obtain the following lower bound on the uplink rate $R_U^{[kl]}$

$$\begin{aligned}
R_U^{[kl]} &= I\left(\hat{x}^{[kl]}; \mathbf{y}_l \mid \sqrt{\rho_r} \sum_{v=1}^L \omega_l^{[kv]} \mathbb{E}[\hat{\mathbf{g}}_v^{[kv]\dagger} \hat{\mathbf{g}}_v^{[kl]}]\right) \\
&\geq \log_2 \left(1 + \frac{\rho_r \left| \sum_{v=1}^L \omega_l^{[kv]} \mathbb{E}[\hat{\mathbf{g}}_v^{[kv]\dagger} \hat{\mathbf{g}}_v^{[kl]}] \right|^2}{\text{Var}[Q_1] + \text{Var}[Q_2] + \text{Var}[Q_3] + \text{Var}[Q_4] + \text{Var}[Q_5]} \right)
\end{aligned}$$

Below we find the variances of Q_1, \dots, Q_5 .

The term Q_1 is caused by the uncertainty of l -the base station about the affective channel $\hat{\mathbf{g}}_l^{[kl]} \hat{\mathbf{g}}_l^{[kl]}$. Since $\hat{\mathbf{g}}_v^{[ks]}$ and $\hat{\mathbf{g}}_r^{[ni]}$ are uncorrelated for any k, s, n, i , using (37), we get

$$\begin{aligned}
\text{Var}[Q_1] &= \rho_r \mathbb{E}[|s^{[kl]}|^2] \sum_{v=1}^L \text{Var}[\hat{\mathbf{g}}_v^{[kv]} \hat{\mathbf{g}}_v^{[kl]}] \\
&= \rho_r M \sum_{v=1}^L |\omega_l^{[kl]}|^2 \frac{\rho_r \tau \beta_v^{[kv]^2}}{1 + \sum_{s=1}^L \rho_r \tau \beta_v^{[ks]}} \cdot \frac{\rho_r \tau \beta_v^{[kl]^2}}{1 + \sum_{s=1}^L \rho_r \tau \beta_v^{[ks]}}.
\end{aligned}$$

Term Q_2 is caused by the pilot contamination. In order to find $\text{Var}[Q_2]$ we note that $s^{[nj]}$ and $s^{[mv]}$ are independent if $(n, j) \neq (m, v)$ and that $\hat{\mathbf{g}}_v^{[nj]}$ and $\hat{\mathbf{g}}_v^{[mv]}$ are uncorrelated if $n \neq m$. Now, using (30) and (37), we obtain

$$\begin{aligned}
&\text{Var}[Q_2] \\
&= \rho_r \sum_{v=1}^L \sum_{\substack{j=1 \\ j \neq l}}^L \sum_{\substack{r=1 \\ r \neq v}}^L \omega_l^{[kv]} \omega_l^{[kr]\dagger} \mathbb{E}[\hat{\mathbf{g}}_v^{[kv]^2} \hat{\mathbf{g}}_v^{[kv]}] \mathbb{E}[\hat{\mathbf{g}}_r^{[kj]^2} \hat{\mathbf{g}}_r^{[kj]}] \\
&\quad + \rho_r \sum_{v=1}^L \sum_{\substack{j=1 \\ j \neq l}}^L |\omega_l^{[kv]}|^2 \mathbb{E}[\hat{\mathbf{g}}_v^{[kv]^2} \hat{\mathbf{g}}_v^{[kj]} \hat{\mathbf{g}}_v^{[kj]^2} \hat{\mathbf{g}}_v^{[kv]}] \\
&= \rho_r \sum_{\substack{j=1 \\ j \neq l}}^L \left| \sum_{v=1}^L \frac{M \rho_r \tau \beta_v^{[kv]} \beta_v^{[kj]}}{1 + \sum_{s=1}^L \rho_r \tau \beta_v^{[ks]}} \omega_l^{[kv]} \right|^2 \\
&\quad + \rho_r M \sum_{\substack{j=1 \\ j \neq l}}^L \sum_{v=1}^L \frac{\rho_r \tau \beta_v^{[kj]^2}}{1 + \sum_{s=1}^L \rho_r \tau \beta_v^{[ks]}} \cdot \frac{\rho_r \tau \beta_v^{[kv]^2}}{1 + \sum_{s=1}^L \rho_r \tau \beta_v^{[ks]}} \\
&\quad \cdot |\omega_l^{[kv]}|^2
\end{aligned}$$

Consider term Q_3 . In the asymptotic regime, as M tends to infinity, the normalized inner-product of $\hat{\mathbf{g}}_v^{[kv]}$ and $\hat{\mathbf{g}}_v^{[nj]}$ almost surely tends to zero since for $n \neq k$ these vectors are independent. For finite M , however, we can not ignore the interference caused by Q_3 . To compute Q_3 we use the

same fact as we used for Q_2 and, using (30), obtain

$$\begin{aligned} \text{Var}[Q_3] &= \rho_r \sum_{v=1}^L \sum_{j=1}^L \sum_{\substack{n=1 \\ n \neq k}}^K |\omega_i^{[kv]}|^2 \text{Tr} \left(\mathbb{E}[\hat{\mathbf{g}}_v^{[kv]} \hat{\mathbf{g}}_v^{[kv]\dagger}] \mathbb{E}[\hat{\mathbf{g}}_v^{[nj]} \hat{\mathbf{g}}_v^{[nj]\dagger}] \right) \\ &\quad \cdot \mathbb{E}[|s^{[nj]}|^2] \\ &= \rho_r M \sum_{v=1}^L \sum_{j=1}^L \sum_{\substack{n=1 \\ n \neq k}}^K |\omega_i^{[kv]}|^2 \frac{\rho_r \tau \beta_v^{[kv]^2}}{1 + \sum_{s=1}^L \rho_r \tau \beta_v^{[ks]}} \\ &\quad \cdot \frac{\rho_r \tau \beta_v^{[nj]^2}}{1 + \sum_{s=1}^L \rho_r \tau \beta_v^{[ks]}}. \end{aligned}$$

Term Q_4 is caused by the estimation error $\tilde{\mathbf{g}}_v^{[nj]}$. Taking into account that in the case of MMSE estimation the estimate $\hat{\mathbf{g}}_v^{[nj]}$ and estimation error $\tilde{\mathbf{g}}_v^{[nj]}$ are uncorrelated, and using (30) and (29), we obtain

$$\begin{aligned} \text{Var}[Q_4] &= \rho_r \sum_{v=1}^L \sum_{j=1}^L \sum_{n=1}^K |\omega_i^{[kv]}|^2 \text{Tr} \left(\mathbb{E}[\hat{\mathbf{g}}_v^{[kv]} \hat{\mathbf{g}}_v^{[kv]^2}] \mathbb{E}[\tilde{\mathbf{g}}_v^{[nj]} \hat{\mathbf{g}}_v^{[nj]^2}] \right) \\ &\quad \cdot \mathbb{E}[|s^{[nj]}|^2] \\ &= \rho_r M \sum_{v=1}^L \sum_{j=1}^L \sum_{n=1}^K |\omega_i^{[kv]}|^2 \frac{\rho_r \tau \beta_v^{[kv]^2}}{1 + \sum_{s=1}^L \rho_r \tau \beta_v^{[ks]}} \\ &\quad \cdot \left(\beta_v^{[nj]} - \frac{\rho_r \tau \beta_v^{[nj]^2}}{1 + \sum_{s=1}^L \rho_r \tau \beta_v^{[ns]}} \right). \end{aligned}$$

Finally, term Q_5 is caused by the additive noise at the receivers of base stations. Using the same arguments as above, we obtain

$$\begin{aligned} \text{Var}[Q_5] &= \sum_{v=1}^L |\omega_i^{[kv]}|^2 \text{Tr} \left(\mathbb{E}[\hat{\mathbf{g}}_v^{[kv]} \hat{\mathbf{g}}_v^{[kv]^2}] \mathbb{E}[\mathbf{w}_v \mathbf{w}_v^\dagger] \right) \\ &= M \sum_{v=1}^L |\omega_i^{[kv]}|^2 \frac{\rho_r \tau \beta_v^{[kv]^2}}{1 + \sum_{s=1}^L \rho_r \tau \beta_v^{[ks]}}. \end{aligned}$$

Combining the obtained results finishes the proof. \blacksquare

Acknowledgement The authors would like to thank Carl Nuzman for his help with the proof of Lemma 5.

REFERENCES

- [1] T. L. Marzetta, Multi-cellular wireless with base stations employing unlimited numbers of antennas, in *Proc. UCSD Inf. Theory Applicat. Workshop*, Feb. 2010.
- [2] L. Li, A. Ashikhmin, T. Marzetta, "Interference Reduction in Massive MIMO Systems II: Downlink Analysis for a Finite Number of Antennas," submitted to *IEEE Trans. on Information Theory*.
- [3] T. L. Marzetta, "Noncooperative Cellular Wireless with Unlimited Numbers of Base Station Antennas," *IEEE Trans. on Wireless Communications*, **9**, pp. 3590–3600, 2010.
- [4] H. Q. Ngo, E. G. Larsson, and T. L. Marzetta, "Energy and spectral efficiency of very largemultiuserMIMOsystems," *IEEE Trans. on Communications*, **61**, pp. 1436-1449, 2013.
- [5] G. Y. Li, Z.-K. Xu, C. Xiong, C.-Y. Yang, S.-Q. Zhang, Y. Chen, and S.-G. Xu, "Energy-efficient wireless communications: Tutorial, survey, and open issues," *IEEE Wireless Commun. Mag.*, **18**, pp. 28-35, 2011.

- [6] C. Xiong, G. Y. Li, S. Zhang, Y. Chen, and S. Xu, "Energy- and spectral- efficiency tradeoff in downlink OFDMA networks," *IEEE Trans. Wireless Commun.*, **10**, pp. 3874-3886, 2011.
- [7] F. Rusek, D. Persson, B. K. Lau, E. G. Larsson, T. L. Marzetta, O. Edfors, and F. Tufvesson, "Scaling up MIMO: Opportunities and challenges with very large arrays," *IEEE Signal Process. Mag.*, **30**, pp. 40-46, 2013.
- [8] E. G. Larsson, F. Tufvesson, O. Edfors, and T. L. Marzetta, "Massive MIMO for next generation wireless systems," *IEEE Commun. Mag.*, **52**, pp. 186-195, 2014.
- [9] Lu Lu ; G. Y. Li, A. L. Swindlehurst, A. Ashikhmin, Rui Zhang, "An Overview of Massive MIMO: Benefits and Challenges," *IEEE Journal of Selected Topics in Signal Processing*, **8**, pp. 742–758, 2014.
- [10] F. Fernandes, A. Ashikhmin, T. L. Marzetta, "Interference Reduction on Cellular Networks with Large Antenna Arrays," *IEEE International Conference on Communications (ICC)*, Ottawa, Canada, 2012.
- [11] F. Fernandes, A. Ashikhmin, T. L. Marzetta, "Inter-Cell Interference in Noncooperative TDD Large Scale Antenna Systems," *IEEE Journal on Selected Areas in Communications*, **31**, pp. 192–201, 2013.
- [12] K. Appaiah, A. Ashikhmin, T. L. Marzetta, "Included in Your Digital Subscription Pilot Contamination Reduction in Multi-User TDD Systems," *International Conference on Communications*, pp. 1–5, 2010.
- [13] J. Hoydis, S. ten Brink, M. Debbah, "Massive-MIMO: How Many Antennas do We Need," *arXiv:1107.1709v2*.
- [14] H. Huh, G. Caire, H.C. Papadopoulos, S.A. Ramprasad, "Achieving "Massive-MIMO" Spectral Efficiency with a Not-so-Large Number of Antennas," *arXiv:1107.3862v2*.
- [15] A. Ashikhmin and T. Marzetta, "Large-Scale Antenna Method And Apparatus Of Wireless Communication With Suppression Of Intercell Interference," *US8774146 patent*, filed on Dec. 19, 2011, Issued on July 8, 2014.
- [16] A. Ashikhmin and T. L. Marzetta, "Pilot contamination precoding in multi-cell large scale antenna systems," *Proceedings of 2012 IEEE International Symposium on Information Theory (ISIT)*, pp. 1137–1141, 2012.
- [17] H. Yang, T. L. Marzetta, "Total energy efficiency of cellular large scale antenna system multiple access mobile networks," *IEEE Online Conference on Green Communications (GreenCom)*, pp.27–32, 2013.
- [18] S. M. Kay, *Fundamentals of Statistical Signal Processing. I: Estimation Theory*, Prentice Hall PTR, 1993.
- [19] J. Jose, A. Ashikhmin, T. L. Marzetta, S. Vishwanath, "Pilot Contamination and Precoding in Multi-Cell TDD Systems," *IEEE Transactions on Wireless Communications*, vol. 10, pp. 2640 – 2651, 2011.
- [20] M. K. Karakayali, G. J. Foschini, R. A. Valenzuela, and R. D. Yates, On the maximum common rate achievable in a coordinated network, *IEEE International Conf. of Commun.*, vol. 9, pp. 4333 - 4338, Jun. 2006.
- [21] M. K. Karakayali, G. J. Foschini, R. A. Valenzuela, Network coordination for spectrally efficient communications in cellular systems, *IEEE Trans. Wireless Commun.*, vol. 13, no. 4, pp. 56 - 61, Aug. 2006.
- [22] G. J. Foschini, M. K. Karakayali, and R. A. Valenzuela, Coordinating multiple antenna cellular networks to achieve enormous spectral efficiency, *IEE Proc. Commun.*, vol. 153, no. 4, pp. 548 - 555, Aug. 2006.
- [23] B. Hassibi and B. M. Hochwald, "How much training is needed in multiple-antenna wireless links?" *IEEE Trans. Inf. Theory*, vol. 49, pp. 951963, Apr. 2003.